ABSTRACT

KAMAT, PRATHAMESH SHIVANAND. Energy Storage Integration in Stand Alone Wave Energy Conversion System. (Under the direction of Dr. Subhashish Bhattacharya.)

Ocean energy is emerging as renewable source of energy which can be used for generation of electricity for a number of applications. One such application can be a stand-alone wave energy generation. Electricity can be generated at the stator terminals of permanent magnet synchronous generator (PMSG) with the use of efficient wave energy converters (WEC) to rotate the turbine and suitable mechanical gear arrangement. Since this power is oscillatory in nature due to oscillatory waves, it cannot be directly fed to a load or grid. Hence it is necessary to integrate the system with appropriate energy storage system (ESS) in order to generate smooth power. This thesis represents a simple approach of integrating hybrid energy storage by the use of battery and supercapacitor along with PMSG for wave energy generation. Wave nature is assumed to be sinusoidal and it is given as speed reference to a 3-phase induction machine which is coupled with PMSG. The overall system is simulated in MATLAB and implemented in hardware to demonstrate the smoothing of power.

Energy Storage Integration in Stand Alone Wave Energy Conversion System

by
Prathamesh Shivanand Kamat

A thesis submitted to the Graduate Faculty of
North Carolina State University
in partial fulfillment of the
requirements for the Degree of
Master of Science

Electrical Engineering

Raleigh, North Carolina

2016

APPROVED BY:

Dr. David Lubkeman	Dr. Mesut Baran

Dr. Subhashish Bhattacharya
Chair of Advisory Committee

DEDICATION

To my parents.

BIOGRAPHY

Prathamesh Kamat was born on October 17, 1990 in Mumbai (Maharashtra), India. He did his schooling from VPM Vidya Mandir, Dahisar, Mumbai. He graduated from Sardar Patel College of Engineering, Mumbai with a Bachelor in Electrical Engineering in 2012. Prathamesh was an Executive Engineer in Air Insulated Switchgear (AIS) Medium Voltage (MV) Business Unit at Siemens India from 2012-2014. He worked on research and development department for design modifications of MV Vacuum Circuit Breakers at Siemens. Many of his responsibilities included the design to order and development of the product based on site complaints.

He joined North Carolina State University in Fall 2014 for M.S. in Electrical Engineering with specialization in Power Systems and Power Electronics. Since Dec 2014, he has been associated with Future Renewable Electrical Energy Delivery and Management (FREEDM) Systems Center during his study at North Carolina State University. His research focuses on stand alone low-cost wave energy generation and energy storage integration

ACKNOWLEDGEMENTS

I am sincerely thankful to my advisor, Dr. Subhashish Bhattacharya for the guidance he has provided me during my graduate program at North Carolina State University. Dr. Bhattacharya has been always helpful and he gave me excellent opportunity to work on wave energy generation and control project.

I thank Dr. David Lubkeman for accepting to become a member of the committee. I am thankful all the help and guidance in the coursework which motivated me in my thesis.

I thank Dr. Mesut Baran for accepting to become a member of the committee. I am thankful for your valuable advice and teaching.

I thank Samir Hazra for his excellent mentorship throughout my masters program. You gave me wonderful opportunity to apply the knowledge of power electronics by making me involved in various kinds of hardware as well as software tasks in your project. Those inspired me to learn power electronics in depth and also enhanced my skills. The knowledge needed for executing this thesis work wouldn't have been possible without your guidance and support.

I thank FREEDM Systems Center for sharing the resources for this project.

I thank ABB for providing funding and for an opportunity to develop the hardware and use it as a part of this thesis.

I thank Swaroop Mohapatra for motivating me in my tough times and helping me to achieve my thesis successfully.

I thank Ashish Shrivastav for his support, suggestions and support throughout the project work and coursework. I also appreciate the valuable suggestions from seniors and friends, Ankan De, Sachin Madhusudan, Krishna Mainali, Awneesh Tripathi, Ritwik Chattopadhyay, Kasu Naidu, Anirudha Mahajan, Abhay Negi, Akshat Yadav and Ganapati Pai at FREEDM Systems Center.

I extend my gratitude towards Karen Autry for always cheering me up.

I thank Hulgize Kassa for his help with electrical equipment as well as supervision assuring my safety in the laboratory.

I thank Anish, Rohit, Ameya, Pratik, Yaman, Ronak, Nivedhitha, Vaishnavi, Ashish Subramnium, Wasim, Utkarsh, Ayush for their support and contribution in my learning.

Finally, I would like to thank my family members, Mom and Dad for their love and support in my happy as well as tough moments during my masters.

TABLE OF CONTENTS

LIST OF TABLES . . . . . **vii**

LIST OF FIGURES . . . . . **viii**

Chapter 1 Introduction **1**

Chapter 2 System Architecture **5**

Chapter 3 Control and Simulation **8**
3.1 Model and Controller Design 9
3.1.1 ESS Current Controller Design 9
3.1.2 ESS Voltage Controller Design 10
3.1.3 Rectified Current Controller Design 12
3.2 Simulation Results 13
3.2.1 ESS Current Control Model 13
3.2.2 ESS Voltage Control Model 15
3.2.3 Rectified Current Control Model 16
3.2.4 System Model With Voltage Source as ESS 19

Chapter 4 Hardware Implementation **20**
4.1 Hardware Setup 20
4.2 Experimental Investigation 23
4.2.1 ESS Current Controller Test 23
4.2.2 ESS Voltage Controller Test 24
4.2.3 Rectifier Current Controller Test 24
4.2.4 PMSG operation using ABB ACS800 drive 26
4.2.5 System Setup With DC Supply as ESS 27
4.2.6 Self excitation for PMSG 27
4.2.7 Real time simulation using NI Labview and CompactRIO 29

Chapter 5 Hybrid Energy Storage **30**
5.1 Supercapacitor 30
5.2 Supercapacitor charging and discharging 31
5.2.1 Constant Current Constant Voltage control 31
5.2.2 Simulation result for charging and discharging of supercapacitor 33
5.2.3 Hardware results for charging and discharging of supercapacitor 34
5.3 System with supercapacitor 34
5.3.1 Simulation Results for System with Supercapacitor 34
5.3.2 System model hardware implementation using supercapacitor 36
5.4 Hybrid energy storage 36
5.4.1 Difference between supercapacitor and battery 36
5.4.2 Need for hybrid control 37

5.4.3 Control and simulation of battery current 38
5.4.4 System model simulation of hybrid supercapacitor and battery control . . 41
5.4.5 System model hardware implementation using hybrid supercapacitor and battery control 43
5.5 Conclusion 45

References **46**

LIST OF TABLES

Table 4.1 System parameters 21
Table 4.2 Voltage Compensation of PMSG using self-excitation capacitors 28

Table 5.1 Supercapacitor Specifications 30

LIST OF FIGURES

Figure 1.1 Schematic of the emulating system . . . 2
Figure 1.2 Hardware setup for emulating WEC . . . 2
Figure 1.3 Sinusoidal speed reference and PMSG terminal voltage . . . 3
Figure 1.4 Wave energy generation for grid application . . . 3
Figure 1.5 Wave energy generation for stand-alone application . . . 4

Figure 2.1 System Block Diagram . . . 5
Figure 2.2 System control structure . . . 6

Figure 3.1 System power circuit with ESS . . . 9
Figure 3.2 I_{ess} control bode plot . . . 10
Figure 3.3 V_{dc} control bode plot . . . 11
Figure 3.4 I_{rect} control bode plot . . . 12
Figure 3.5 Model for ESS current controller test . . . 13
Figure 3.6 ESS current controller . . . 14
Figure 3.7 ESS current plot . . . 14
Figure 3.8 Model for ESS voltage controller test . . . 15
Figure 3.9 ESS voltage controller . . . 15
Figure 3.10 ESS current plot . . . 16
Figure 3.11 DC bus voltage plot . . . 16
Figure 3.12 Model for rectifier current controller test . . . 17
Figure 3.13 Rectifier current controller . . . 17
Figure 3.14 Rectified current i_{rect} plot . . . 18
Figure 3.15 System model with voltage source as ESS . . . 19
Figure 3.16 V_{DC} plot from system model simulation . . . 19

Figure 4.1 System Hardware . . . 22
Figure 4.2 i_{ess} controller test in hardware . . . 23
Figure 4.3 i_{ess} controller test in hardware plots . . . 24
Figure 4.4 V_{DC} controller test in hardware Ch1: DC Bus Voltage V_{DC} controlled at 50V, Ch2: Reference current i_{essref} (A), Ch3: Measured inductor current i_{ess} (A) . 25
Figure 4.5 i_{GEN} controller test in hardware Ch1: Actual inductor current i_{rect} (A), Ch2: Reference current $i_{rectref}$ (A), Ch3: Measured inductor current i_{rect} (A) . . . 25
Figure 4.6 PMSG terminal voltage and speed reference, Ch1: Stator line voltage V_{ab} (Scale 1V=3V), Ch2: Rectified voltage V_{rect} (1V), Ch1: Stator line voltage V_{bc} (Scale 1V=3V) . . . 26
Figure 4.7 System with ESS test in hardware Ch1: DC Bus Voltage V_{DC} controlled at 50V, Ch2: Supercapacitor boost inductor current i_{SC} (A), Ch3: Rectifier boost inductor current i_{Rect} (A) . . . 27
Figure 4.8 Self-excitation capacitor connection for PMSG . . . 28
Figure 4.9 Buoy CRIO model in NI Labview . . . 29
Figure 4.10 Labview and machine model in NI Labview . . . 29

Figure 5.1 Maxwell 48V supercapacitor module 31
Figure 5.2 V_{sc} control bode plot 32
Figure 5.3 Supercapacitor charging schematic 33
Figure 5.4 Constant current and constant voltage logic 34
Figure 5.5 Plots for system model with supercapacitor of 30V 35
Figure 5.6 Supercapacitor charging-discharging test in hardware Ch1: Supercapacitor Voltage V_{SC} controlled at 10V, Ch2: SC boost inductor reference current i_{SCref} (A), Ch3: SC boost inductor current i_{SC} (A) 36
Figure 5.7 System with supercapacitor test in hardware Ch1: SC boost inductor current i_{SC} (1V=1A), Ch1: Ch2: Rectifier boost inductor current i_{Rect} (1V=1A), Ch3: DC Bus Voltage V_{DC} (V) 37
Figure 5.8 I_b control bode plot 39
Figure 5.9 v_{sc} control bode plot 40
Figure 5.10 System circuit with hybrid battery and supercapacitor 41
Figure 5.11 Plots for system model with hybrid battery and supercapacitor control 42
Figure 5.12 Hybrid battery and supercapacitor controller 43
Figure 5.13 Hardware setup for wave energy generation with hybrid energy storage . . . 44
Figure 5.14 System with hybrid energy storage test in hardware Ch1: Supercapacitor current I_{SC} (1V=1A), Ch2: Battery current I_b (1V=1A) Ch3: Rectifier current I_{Rect} (1V=1A), Ch4: Load current I_{Rect} (1V=1A) 44

Chapter 1

Introduction

Ocean energy is emerging as renewable source of energy which can be used for generation of electricity. It can serve as a cost effective solution for providing power to the navy applications. Compared to solar and wind power generation, ocean wave energy is yet to gain the popularity. But researches are being carried to find efficient and economical solutions for generating power using wave energy.

Several wave energy converter (WEC) designs have been made in order to harvest maximum energy from ocean wave [1]. Out of those, point absorber buoy and paddle based WEC systems drive generator directly to provide power [2]-[4]. By use of efficient WEC, wave energy generated can be used in grid application or stand-alone application.

Research also has been done on designing a WEC dynamic model in [16]. In this, WEC mechanism is also emulated based on the dynamic equations. The overall system diagram for emulation is shown in the Fig. 1.1. Ocean wave can be considered as combination of several low frequency sinusoidal waves. Buoy dynamics and wave nature can be emulated using NI labview and real-time simulator CompactRIO to generate necessary torque command signal for drive. Hardware setup can be developed as shown in Fig.1.2 [16]. Sinusoidal speed reference can also be generated by using this setup as shown in Fig. 1.3 [16]. In this thesis, single sinusoidal wave with a period of 10 sec is considered for simplicity. This reference command is given to the drive by DSP using appropriate scale.

Fig. 1.4 shows wave energy generation for grid application [5]. PMSG is connected to the WEC with appropriate gear mechanism. The machine side converter (MSC) controls the power generation by controlling the machine current. The grid side converter (GSC) controls power from the dc bus and dispatches it to the grid. It regulates the dc bus voltage and also it can

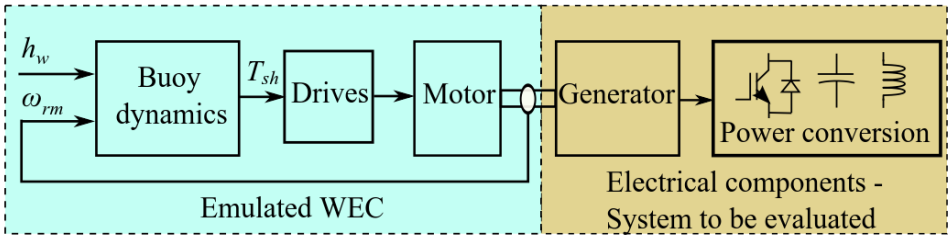

Figure 1.1: Schematic of the emulating system

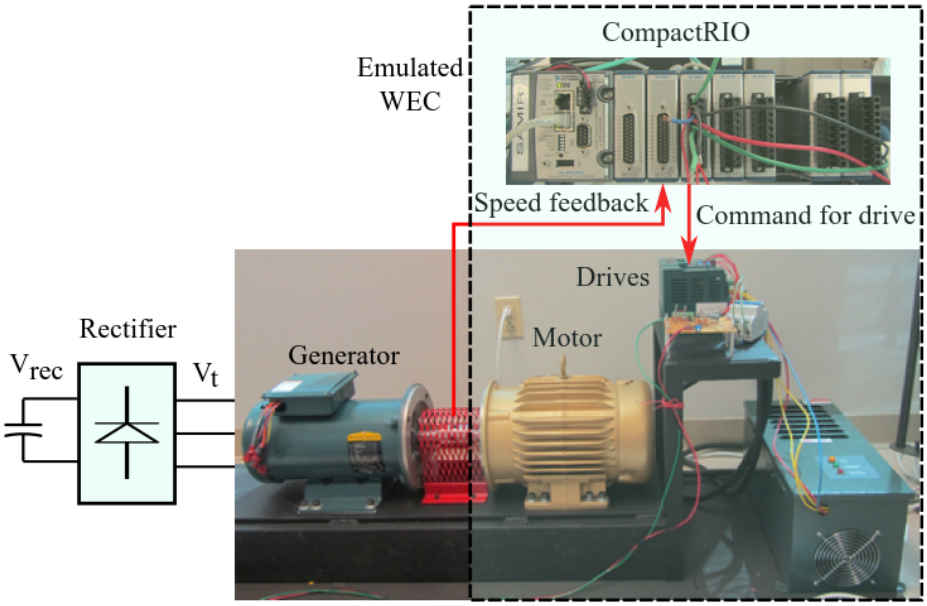

Figure 1.2: Hardware setup for emulating WEC

generate reactive power for the grid if required. Line filters are installed in order to bring down the line current ripple to an acceptable range. A line frequency transformer can interface the whole unit of WECS with the grid. Transformer provides galvanic isolation as well as necessary voltage step up to connect the system with the grid.

Fig. 1.5 shows wave energy generation for grid application [6]. The PMSG which is connected to the WEC generates oscillatory power. PMSG output power is then rectified using AC-DC converter. It is passed through DC-DC boost converter and connected to a stand-alone resistive load. Energy storage system is connected to the load through a bi-directional DC-DC converter.

Various design approaches for power smoothing using hybrid energy storage are made in mi-

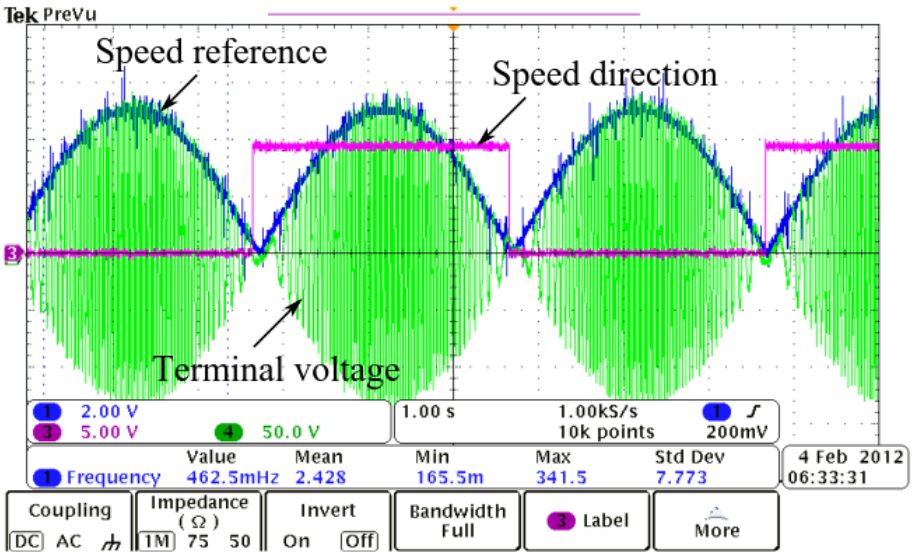

Figure 1.3: Sinusoidal speed reference and PMSG terminal voltage

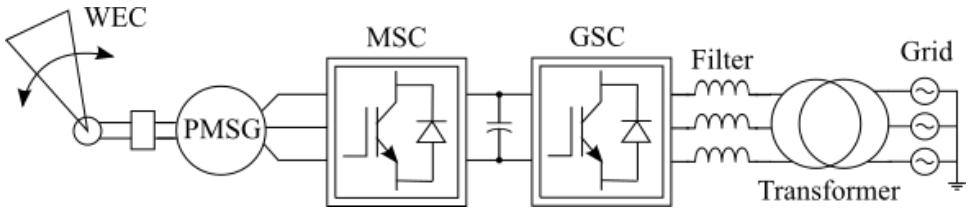

Figure 1.4: Wave energy generation for grid application

crogrid system [7], wind energy generation [8] and electric vehicles [9]. Ocean wave is oscillatory in nature and hence generates oscillatory power. To provide constant power to a stand-alone application, it is necessary to filter out the oscillations using Energy Storage System (ESS).

This thesis focuses on the stand-alone wave energy generation. It discusses about the controller design, model simulation and hardware development which can be done using minimum components. It also proposes the hybrid energy storage system control for better power smoothing. For this purpose; permanent magnet synchronous generator (PMSG), AC Drive, DC-DC power converter, supercapacitor, DC power supply and a stand-alone resistive load bank is used.

Chapter 2 discusses about the system architecture and design which is being used for the study. It explains functionality of the design and how power smoothing can be achieved.

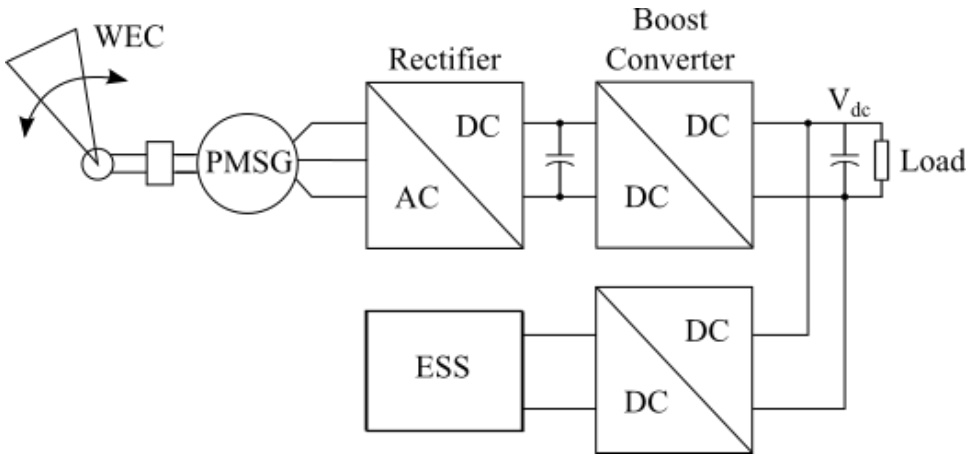

Figure 1.5: Wave energy generation for stand-alone application

Chapter 3 explains the system controller design and model simulation. It includes the transfer functions, controller parameters and bode plot results to show the approach. It also shows the MATLAB models which verify the controller design by model simulation of system blocks. In this chapter, ESS is considered as a single block which works as a power smoothing device.

Chapter 4 is focused on the hardware development and the experimental results which verify the simulation results obtained in chapter 3. It shows the hardware structure built in lab and elaborates the step by step experimenting process to be carried out as we are building the system.

Chapter 5 deals with the use of supercapacitor and battery as energy storage devices. It explains the charging and discharging of supercapacitor. Specific reasons for the need of hybrid energy storage devices are also discussed. Entire system architecture is implemented using these energy devices and hardware results are compared with that of the simulation.

Chapter 2

System Architecture

Research has been done on wave energy generation for stand-alone application in [6] and similar design approach is used in this thesis. The system design used is as shown in the Chapter 1 Fig. 1.5.

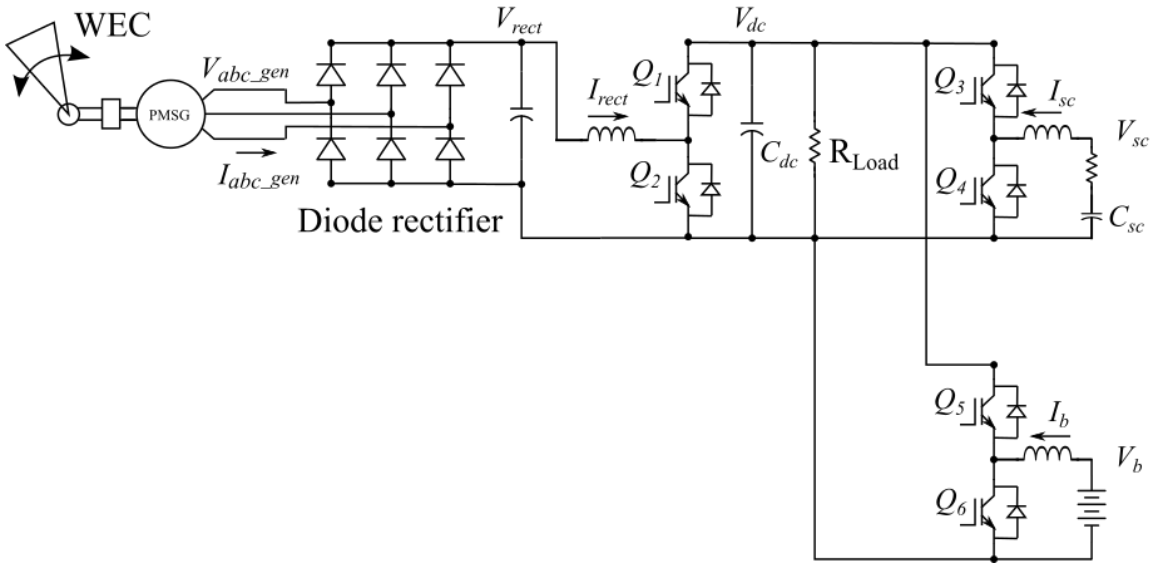

Figure 2.1: System Block Diagram

The power circuit used for the system is as shown in Fig. 2.1. The voltage output is rectified by a diode rectifier bridge. Supercapacitor and battery are used as energy storage devices. For maintaining the constant power for stand-alone application, it is necessary to control DC bus voltage and individual powers from generator and energy storage systems. DC bus voltage is regulated by supercapacitor side DC-DC boost converter. Output DC bus voltage is generally controlled at a value higher than the rectified voltage. Another boost converter is used to control the rectified current. This current is controlled to generated optimum power from PMSG. Rectifier current reference is generated proportional to the WEC speed reference. This assumption is necessary because output impedance of the system needs to be equal to its source impedance in order to generate optimal power [6].

Thus, overall system control is achieved by controlling the current flow from rectifier, supercapacitor and battery. Supercapacitor boost converter is used to control DC bus voltage and to provide peak power requirement. Battery can charge or discharge with suitable control in order to provide average power mismatch and also limit supercapacitor terminal voltage. This controol strategy will be discussed in later chapters in detail. In any case, ESS power is controlled in such a way that load should always get constant power. ESS will charge or discharge whenever generated power is above or below average load power respectively.

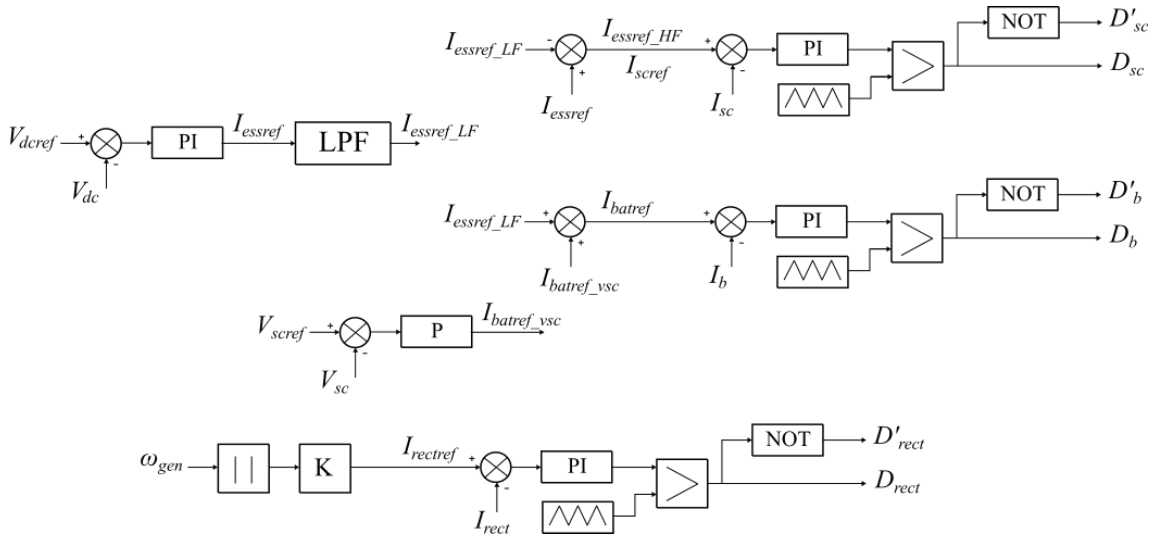

Figure 2.2: System control structure

Fig. 2.2 shows the control circuit for the system power circuit. There are three current controllers and two voltage controllers used in the system. This control structure can be explained in brief as follows. Rectifier current reference $I_{rectref}$ is proportional to the absolute value of the generator speed ω_{gen}. It is compared with the actual rectifier current I_{rect} to generate duty cycle for rectifier boost converter. Supercapacitor side boost converter the DC bus voltage V_{dc} using a PI controller and it generates equivalent ESS reference current I_{essref}. This ESS reference current has a high frequency component over an average component. Appropriate low pass filter (LPF) is used to split the I_{essref} into high frequency component I_{essref_HF} and low frequency component I_{essref_LF}. High frequency component is compared with actual supercapacitor current I_{sc} to generate duty cycle for supercapacitor boost converter. Low frequency component contributes to the battery reference current. Another reference for battery current is computed from the voltage controller which controls supercapacitor terminal voltage V_{sc}. This is a precaution taken to avoid overcharging or over-discharging of the supercapacitor which can result in the system failure. Battery reference current I_{batref} is then compared with actual battery current I_b to generate duty cycle for battery boost converter.

Chapter 3

Control and Simulation

Boost converters are designed for 10kHz switching frequency. Maximum DC bus voltage is considered to be 200V. Given ripple in current, inductance can be found as

$$L = \frac{V_{in} D T_s}{2\Delta I} \tag{3.1}$$

Consider schematic shown in Fig. 3.1. For ESS side boost converter, considering maximum input voltage of energy storage as $V_{ess} = 50V$ and current maximum as $I = 20A$. Hence for ESS boost converter, L_{ess} is chosen to be 1mH considering 5% current ripple. Similarly; for rectifier boost converter, considering maximum input voltage of rectified voltage as $V_{rect} = 150V$ and current maximum as $I = 10A$. L_{rect} is chosen to be 5mH considering 5% current ripple. Capacitor C_{dc} can be selected to minimize the ripple in output voltage. In this case, 470μF is chosen.

System control design and the modeling is done using MATLAB. Boost converter can be controlled using numerous methods depending upon the control requirement [10]. For simplicity we will first consider ESS as an ideal energy storage device like a constant DC supply which can charge or discharge as required. In this system, our aim is to control the power flow through the PMSG and charging-discharging of the ESS while maintaining the voltage at the DC bus constant. Hence, normal voltage regulator design for the boost won't be sufficient since it will fail to control the current flow. It is necessary to operate the converter in current control mode. A simple approach would be to design separate controllers for current as well as voltage. Since PMSG generated terminal voltage is dependent on the speed of the wave, it is fluctuating in nature ranging from zero to the peak value. Hence ESS side boost converter is suitable for regulating the output voltage at the DC bus.

This results into two current controllers and one voltage controller which are required for

the control of the system. These controllers are as follows.

1. ESS Current Controller
2. ESS Voltage Controller
3. Rectified Current Controller

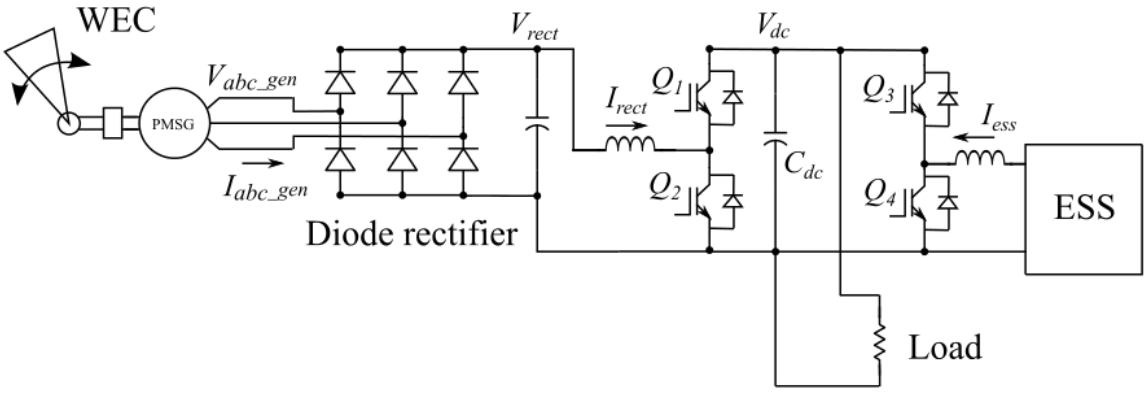

Figure 3.1: System power circuit with ESS

3.1 Model and Controller Design

3.1.1 ESS Current Controller Design

Consider the Fig.3.1 We can write the voltage across the ESS side inductor L_{ess} as

$$d_{ess}V_{dc} - V_{ess} = I_{ess}L_{ess}s \tag{3.2}$$

Here V_{dc} is the output DC voltage which is assumed to be 200V, I_{ess} is the ESS side boost converter inductor current, d_{ess} is the duty ratio of the ESS boost. Since V_{ess} is the disturbance input, the transfer function can be given as follows.

$$G_{I_{ess}}(s) = \frac{I_{ess}(s)}{d_{ess}(s)} = \frac{V_{dc}}{L_{ess}s} \tag{3.3}$$

Switching frequency is 10kHz and targeted bandwidth for current controller is around 1/20th of switching frequency. It was seen that 300Hz bandwidth gave best result for controller. PI

controller is designed and Kp, Ki values are appropriately chosen to achieve 300Hz bandwidth for current i_{ess}.

$$H_{I_{ess}}(s) = \frac{0.00944(s + 2.966)}{s} \tag{3.4}$$

The plant transfer function, controller and closed loop gain bode plot is shown in the Fig. 3.2.

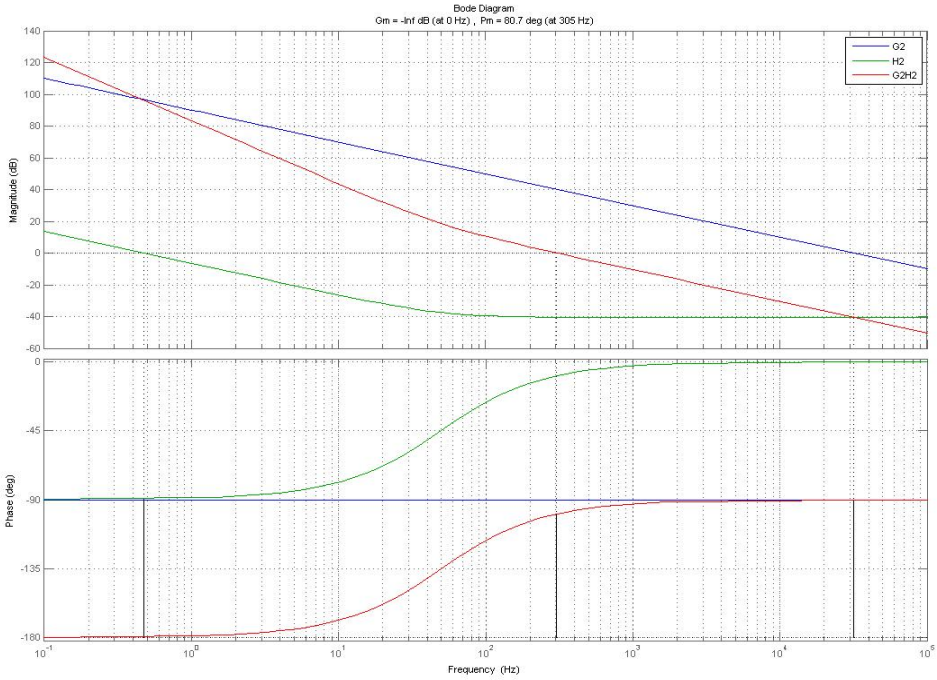

Figure 3.2: I_{ess} control bode plot

3.1.2 ESS Voltage Controller Design

We can write the voltage across the output capacitor C_{dc} as

$$V_{dc}(s) = \frac{I_{dc}(s)}{C_{dc}s}, \tag{3.5}$$

$$V_{dc}(s) = \frac{1 - D_{ess}}{C_{dc}s} I_{essref}(s) \tag{3.6}$$

The transfer function can be given as follows.

$$G_{I_{ess}}(s) = \frac{V_{dc}(s)}{I_{essref}(s)} = \frac{1 - D_{ess}}{C_{dc}s} \tag{3.7}$$

PI controller is designed and Kp,Ki values are appropriately chosen to achieve 45Hz bandwidth for voltage v_{dc}. In this case bandwidth of voltage controller is chosen lesser than the current controller. Since this is acting like a current mode control, current controller needs to be higher than the voltage controller bandwidth.

$$H_{I_{ess}}(s) = \frac{0.531(s + 25.02)}{s} \tag{3.8}$$

The plant transfer function, controller and closed loop gain bode plot is shown in the Fig. 5.2.

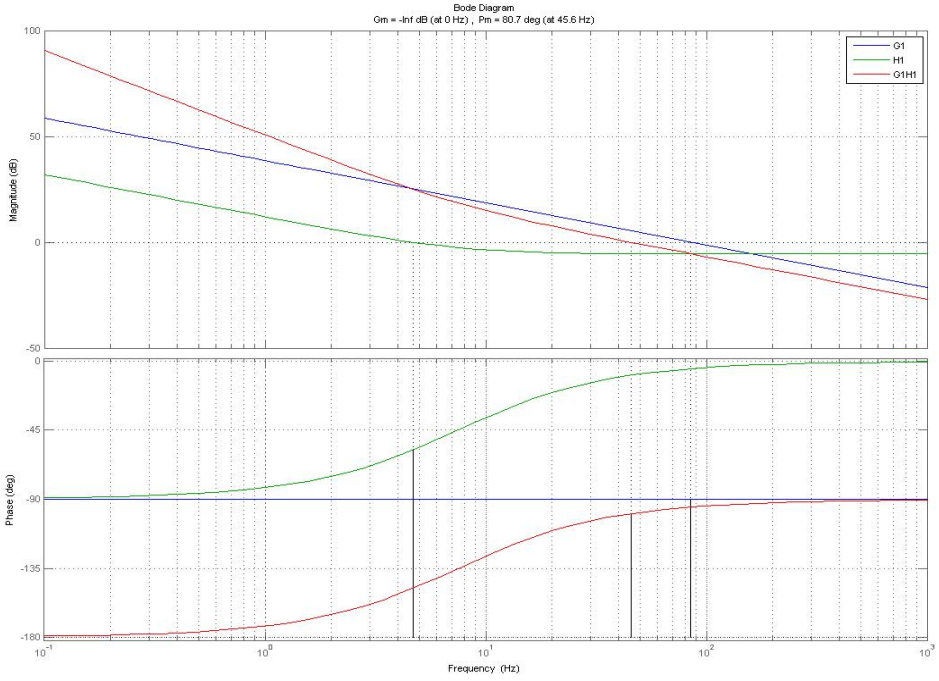

Figure 3.3: V_{dc} control bode plot

3.1.3 Rectified Current Controller Design

We can write the voltage across the rectifier side inductor L_{rect} as

$$d_{rect}V_{dc} - V_{rect} = I_{rect}L_{rect}s \tag{3.9}$$

Here V_{rect} is the diode rectifier output voltage which is dependent on the wave speed reference. I_{rect} is the PMSG side boost converter inductor current, d_{rect} is the duty ratio of the PMSG boost. Since V_{rect} is the disturbance input, the plant transfer function can be given as follows.

$$G_{I_{rect}}(s) = \frac{I_{rect}(s)}{d_{rect}(s)} = \frac{V_{dc}}{L_{rect}s} \tag{3.10}$$

PI controller is designed and Kp, Ki values are appropriately chosen to achieve 300Hz bandwidth for current I_{rect}.

$$H_{I_{rect}}(s) = \frac{0.0473(s + 14.86)}{s} \tag{3.11}$$

The plant transfer function, controller and closed loop gain bode plot is shown in the Fig. 3.4.

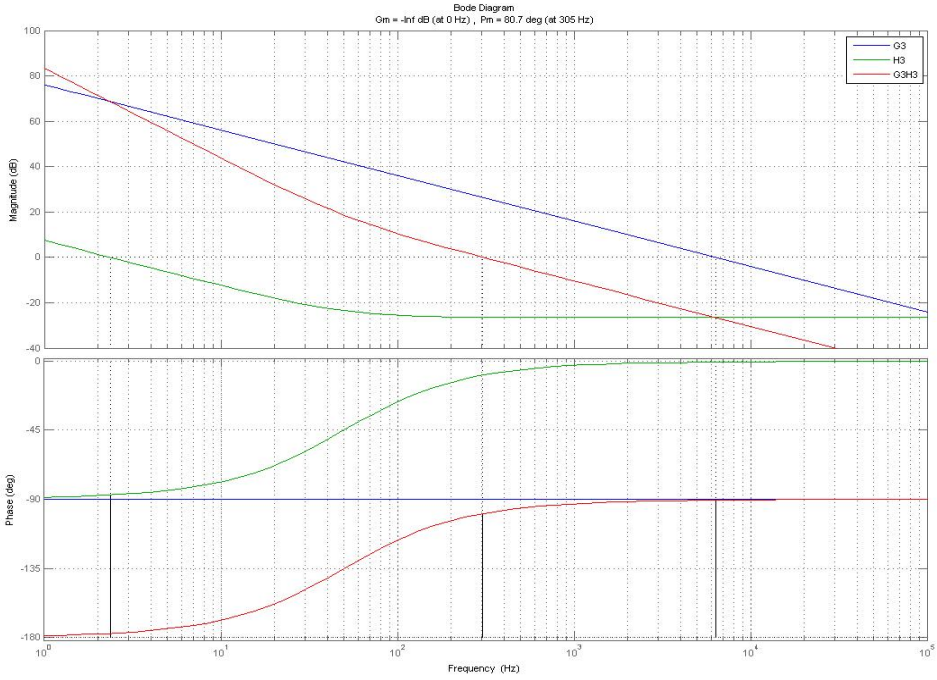

Figure 3.4: I_{rect} control bode plot

3.2 Simulation Results

The system block diagram shown in the Fig. 3.1 is modeled in the MATLAB Simulink. Basic PMSG mathematical model is used to generate the voltage based on the sinusoidal speed reference. Diode rectifier bridge is used from sympower toolbox. Boost converter models are created using single leg converter Real Time - Event toolbox. Controllers are modeled using MATLAB logic blocks with Kp and Ki values obtained in equations 3.4, 3.8 and 3.11. Following subsections show the simulation of individual boost converters and their controllers to ensure the correct operation. This step by step modeling is started by considering ESS side boost converter.

3.2.1 ESS Current Control Model

Energy storage system can be assumed like a constant DC voltage source as shown in Fig. 3.5. Current controller model is shown in the Fig. 3.6. The DC bus voltage is maintained at 200V by DC supply in order to test the current controller. This controller is suitable for controlling the i_{ess} as shown in Fig. 3.7. Current is controlled at 3A as required.

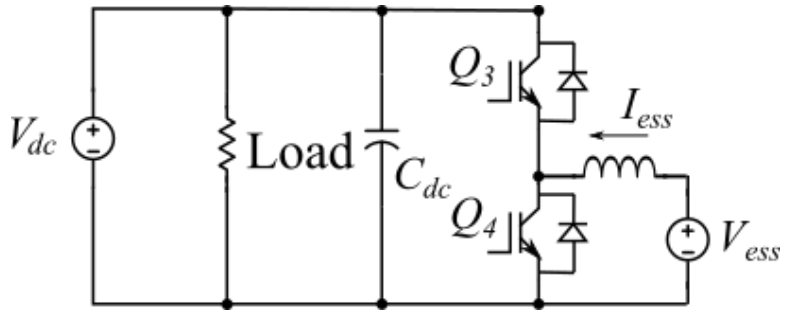

Figure 3.5: Model for ESS current controller test

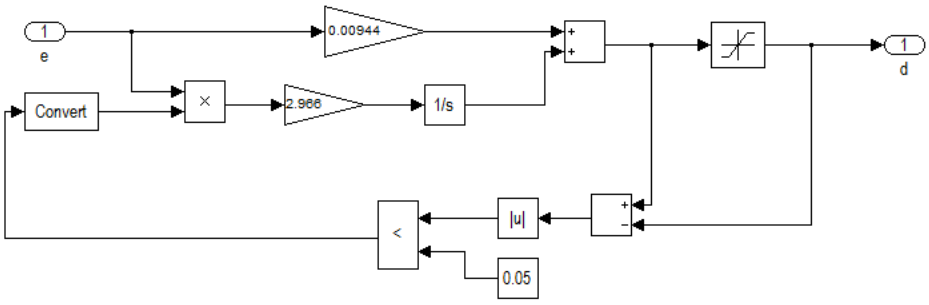

Figure 3.6: ESS current controller

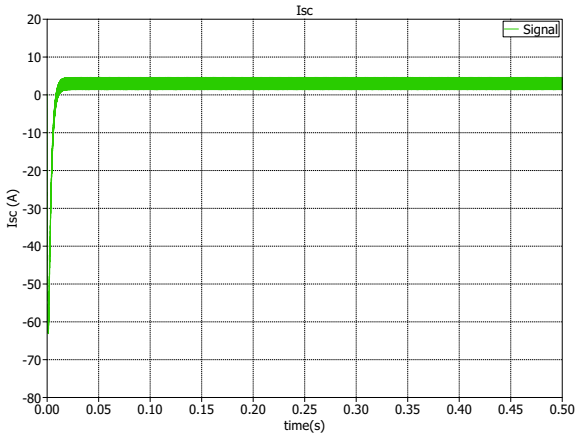

Figure 3.7: ESS current plot

3.2.2 ESS Voltage Control Model

We need to control the charging and discharging of the ESS while maintaining the voltage at the DC bus constant. In other words, when the generated power is greater than the load, the ESS should be in the charging cycle. When the generated power is less than the load, the ESS should be in the discharging cycle. Hence, voltage controller should be able to decide the reference of the ESS current. This is achieved as shown in the Eqn. 3.7. It will be seen in later chapters that this voltage will actually be controlled by supercapacitor boost converter.

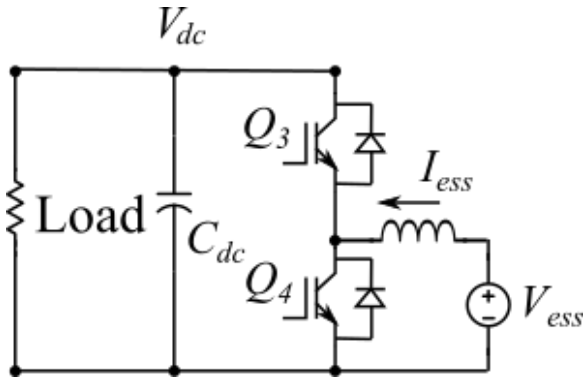

Figure 3.8: Model for ESS voltage controller test

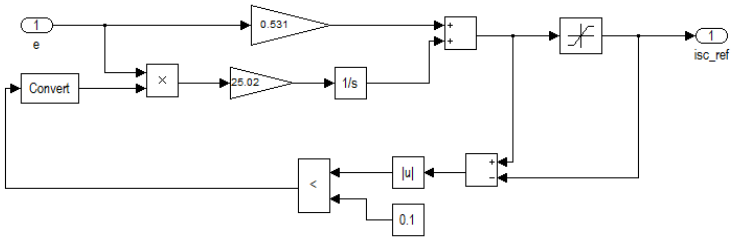

Figure 3.9: ESS voltage controller

As seen in Fig 3.9, the current reference is generated by the voltage controller. Hence we get the ESS boost current as shown in the Fig. 3.10. The voltage is controlled at the desired value of 200V by controlling the ESS boost current as shown in Fig. 3.11. Fig 3.11 also shows that for a sudden load change from 100Ω to 50Ω at 2.5sec, stability of the controller is not affected and voltage is regulated at 200V.

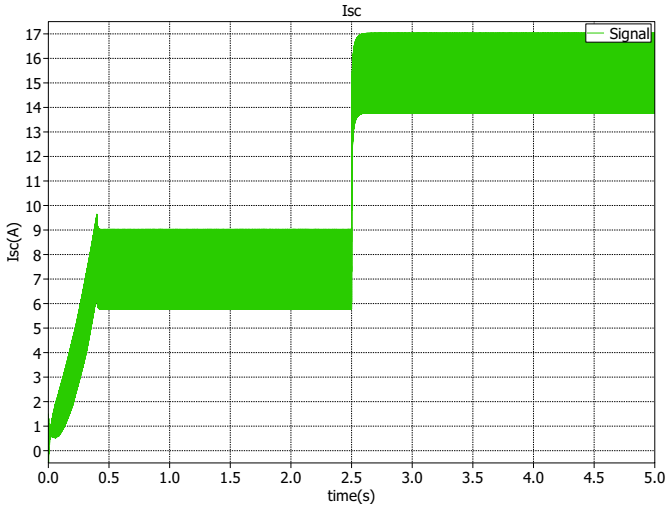

Figure 3.10: ESS current plot

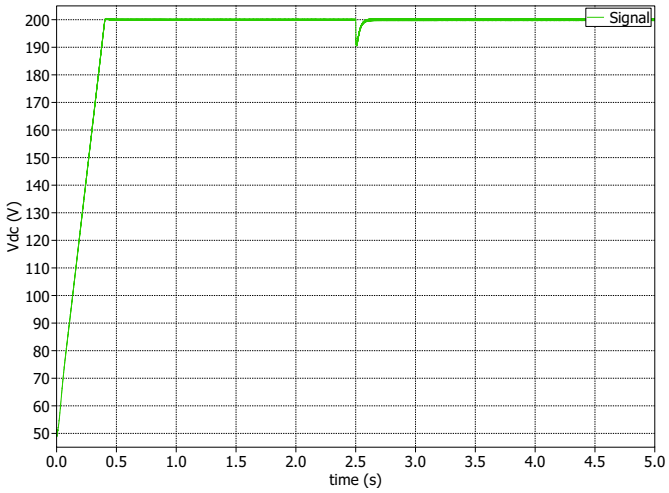

Figure 3.11: DC bus voltage plot

3.2.3 Rectified Current Control Model

Rectified Current Control model is created as shown in the Fig. 3.12. PMSG model generates voltage depending on the speed refernce, which in this case is the sinusoidal wave. Speed input amplitude is varied to get the desired terminal voltage. Diode rectifier rectifies the generated voltage to give the rectified voltage which is the input for the rectifier boost converter. As discussed earlier, rectifier boost current reference is chosen proportional to the absolute value of speed reference for optimum power transfer.

But in this simulation, currrent controller is first test for constant current reference of 3A. It can be modified later to sinusoidal reference once successful operation of controller is achieved. Output DC bus is maintained at 200V using a voltage source as if it is being regulated by ESS side boost converter. This is done to remove the complexity of the models and keep design simple for testing individual controller.

The current controller based on Eqn. 3.10 and Eqn. 3.11 provides the suitable duty cycle to the boost model. Sudden load change from 100Ω to 50Ω at 2.5sec does not affect the stability of the controller and current is regulated at 3A as shown in Fig. 3.14.

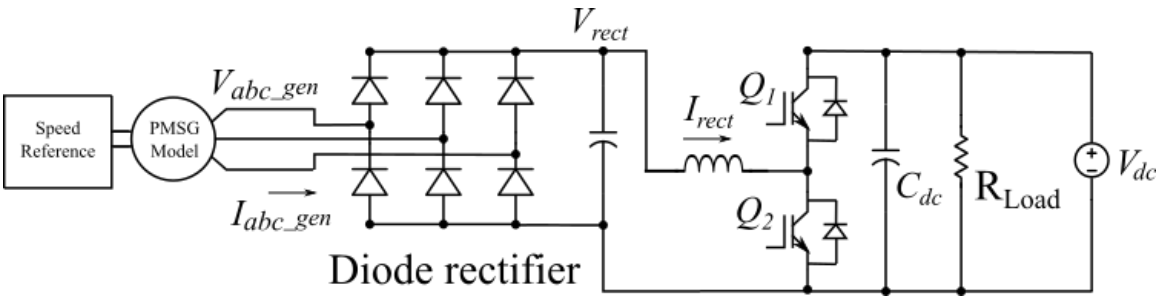

Figure 3.12: Model for rectifier current controller test

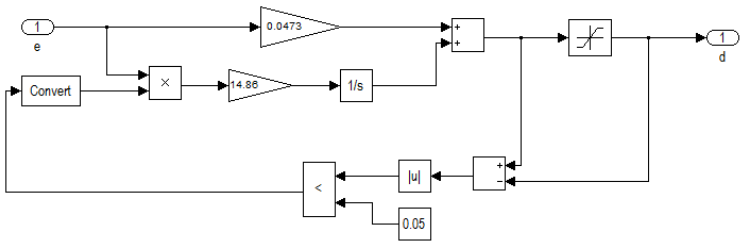

Figure 3.13: Rectifier current controller

Fig. 3.13 shows the controller logic. This controller is suitable for controlling the i_{rect} as shown in Fig. 3.14. It can be seen from the plot that the current is controlled at 3A as required.

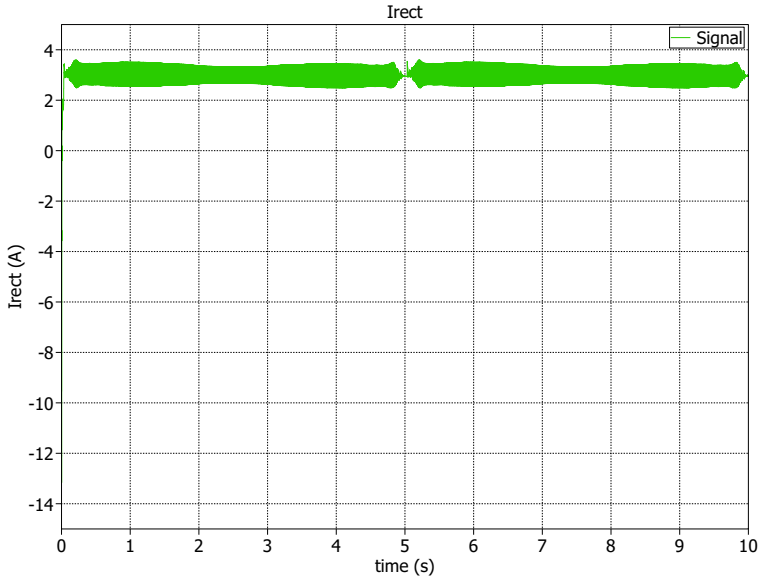

Figure 3.14: Rectified current i_{rect} plot

3.2.4 System Model With Voltage Source as ESS

By combining models in Fig. 3.15 and Fig. 3.12, system model is created. Vdc is maintained at 200V by ESS boost converter. Current reference for rectifier current controller is generated as a multiple of speed reference. Load current is changed from 2A to 12A and load regulation can be seen in 3.16

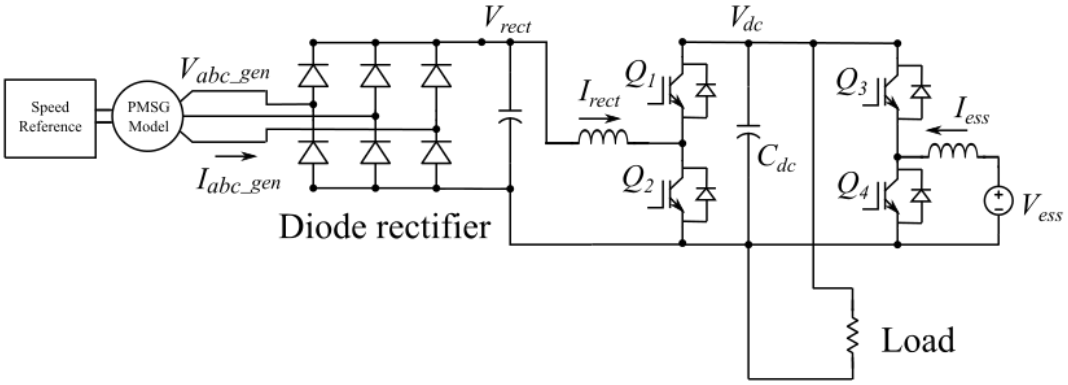

Figure 3.15: System model with voltage source as ESS

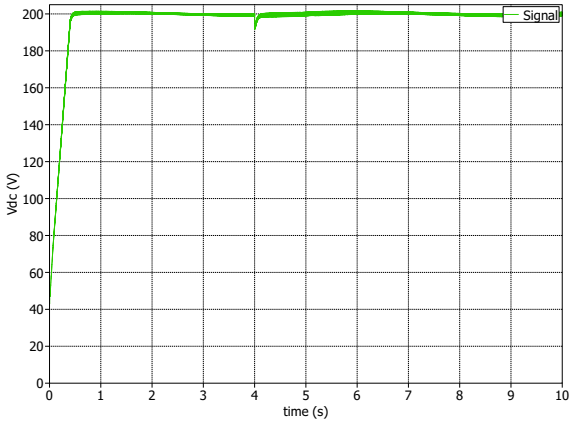

Figure 3.16: V_{DC} plot from system model simulation

Chapter 4

Hardware Implementation

This chapter includes the hardware implementation of the control simulations carried in the Chapter 2. For assuring the system performance, the system is operated with voltage source as ESS.

4.1 Hardware Setup

Hardware setup for the wave energy genearation is shown in Fig. 4.1. Entire setup can be devided into 4 parts.

1. Control circuit
2. Power converter circuit
3. Supercapacitor and battery circuit
4. Motor-generator set

Fig. 4.1a shows the control circuit. Oztek OZDSP3000 control board is used for the entire control in the system. It provides the analog speed reference to the ABB ACS800 drive. It has an important role in sending PWM signals to the power converters. Figure also shows an interface board with flat ribbon cables. This board is used as an interface between control board and power converter. It is used to provide fault protection as well as to receive sensor signals from the voltage sensors and current sensors. Power supply with various output voltages such as 5V, 24V, 15V and -15V is used to power the control board, interface board and other requirements in the system.

Fig. 4.1b shows the power converter circuit. Anti parallel diodes of the MOSFET switches in the inverter circuit are used as diode rectifier. These two inverters can further be used as

Table 4.1: System parameters

Component	Parameters	Value
Induction Motor	Voltage (L-L)	460 V
	Current	4 A
	RPM	1755 rpm
PMSG	Voltage (L-L)	230 V
	Current	8 A
	RPM	1755 rpm
Inductor	L_{rect}	5 mH
	L_{sc}	1 mH
	L_b	1 mH
Capacitor	C_{dc}	470 μ F

active rectifiers for grid application. A separate power converter circuit housed on the left side of the figure is used for boost converters of the rectifier as well as supercapacitor. LEM current sensors are used to provide the current sensing of the rectified current, supercapacitor current.

Fig. 4.1c shows the energy storage system. It shows a supercapacitor used as ESS which will be discussed in the next chapter. Figure also shows two inductors which are used in the boost converter circuit. Figure shows film capacitors which are used for self excitation of the PMSG to improve terminal voltage.

Fig. 4.1d shows the machine hardware. Induction Motor (yellow) is driven by the ABB ACS800 drive with a sinusoidal speed reference generated by the DSP. The PMSG (green) is coupled with the Induction Motor, due to which the former generates voltage at its stator terminals.

All the component ratings are provided in the table 5.1

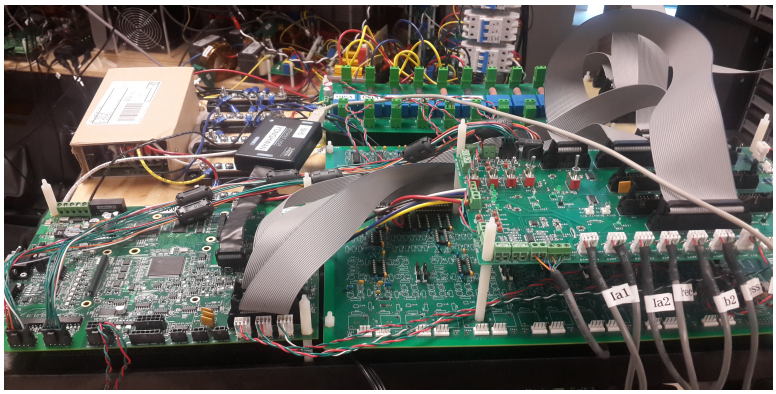

(a) Control Circuit

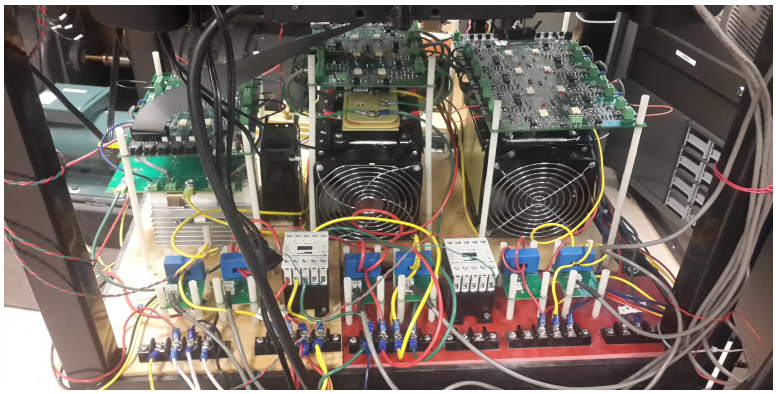

(b) Boost Circuit

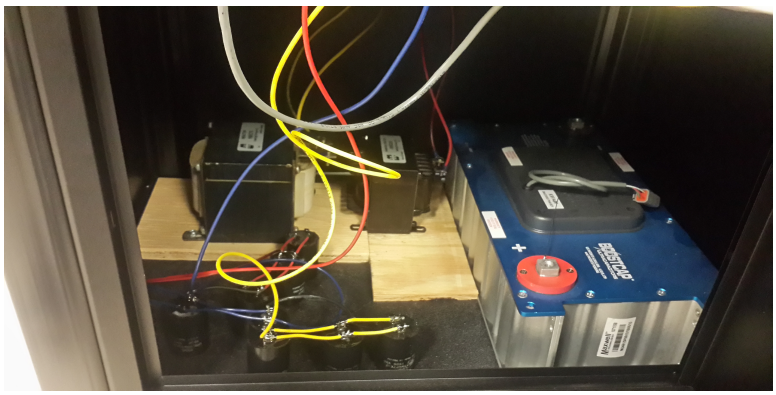

(c) Supercapacitor Circuit

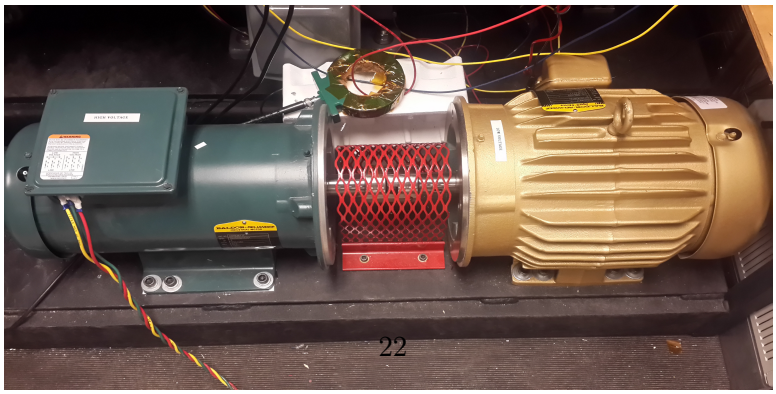

(d) Machine set

Figure 4.1: System Hardware

4.2 Experimental Investigation

The experimental investigation is carried out in a step by step process to achieve the desired end result.

4.2.1 ESS Current Controller Test

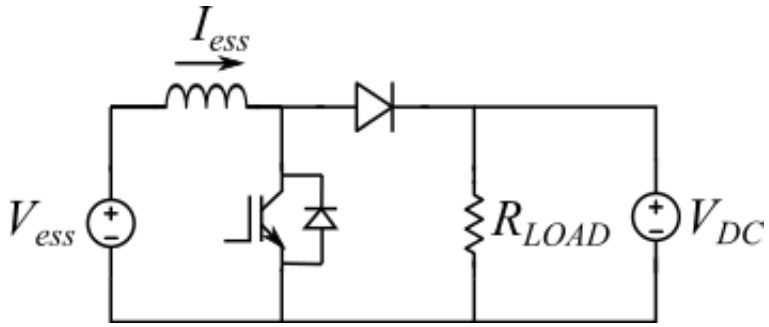

Figure 4.2: i_{ess} controller test in hardware

PWM for the ESS boost converter is generated by the current controller and hence it is necessary to test current controller at first. Since failure of the controller can damage the costly equipment, the controller was tested by applying low voltage input to the ESS boost converter. This experiment is done by keeping DC bus voltage at 75V. Another power supply is used to act as ESS which gives 30V input to the boost converter. As you can see in the Fig. 4.2, R_{LOAD} is connected at the output, which is maintained at 75V by a DC power supply. Since DC supply cannot take in any current or cannot act as a load, it is required to choose optimum value of R_{LOAD}. I_{out} is output current.

$$I_{LOAD} = \frac{V_{DC}}{R_{LOAD}} \tag{4.1}$$

$$I_{out} = I_{ess}(1 - D_{ess}) \tag{4.2}$$

where D_{ess} is the duty cycle of the converter. Load current I_{LOAD} would be actually sum of I_{out} and current from V_{DC}. For a boost converter,

$$\frac{V_{DC}}{V_{ess}} = \frac{1}{1 - D_{ess}} \tag{4.3}$$

For V_{DC} of 75 V and V_{SC} of 30 V, we get D_{ess} of 0.6. R_{LOAD} is chosen as 33 Ω which means I_{LOAD} will be 2.3 A. Now if boost converter provides an output current of value less than 2.3 A,

we can avoid the current from flowing into the DC supply at the DC bus. A current reference of 3 A is given as ESS current reference in DSP program. This results in I_{out} of 1.2 A. I_{LOAD} being sufficiently higher than I_{out}, DC power supply provides positive current. Fig. 4.3 shows the I_{ess} of 3A is achieved.

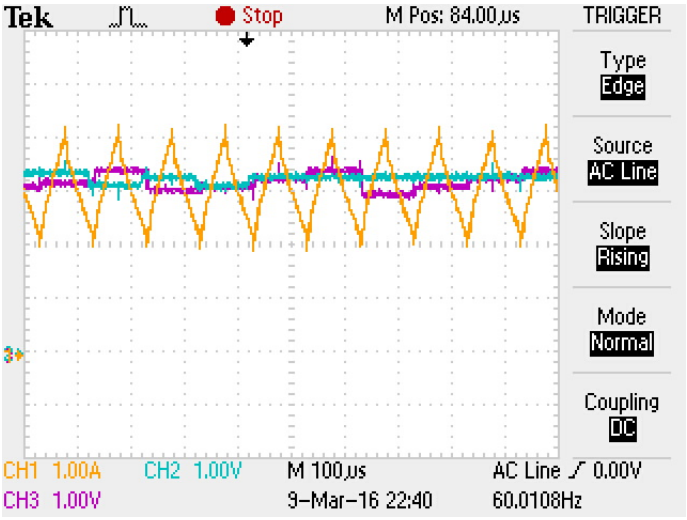

Figure 4.3: i_{ess} controller test in hardware plots

4.2.2 ESS Voltage Controller Test

DC bus voltage needs to be controlled by the voltage controller of ESS boost converter. Again, converter is first tested for low voltage inputs. In this test, V_{ess} is maintained at 30 V by DC power supply. V_{DCref} is 50V. Based on the controller designed in chapter 2 Eqn 3.7 and 3.8, I_{essref} is generated. By this reference, power flow from the DC power supply. Figure 4.4 shows the plot for actual inductor current and reference current. We can conclude from the plots that the voltage as well as the current is controlled by the ESS boost converter.

4.2.3 Rectifier Current Controller Test

In order to experiment the rectified current controller, DC power supply of 30 V is given at the input of the boost converter. Rectifier boost converter inductor current reference $i_{rectref}$ is kept at 2 A. By using the Kp and Ki values obtained from the Chapter 2 Eqn 3.10 and 3.11, the PI control is done by the use of DSP to generate required PWM duty. Figure 4.5 shows the plot for actual inductor current and reference current.

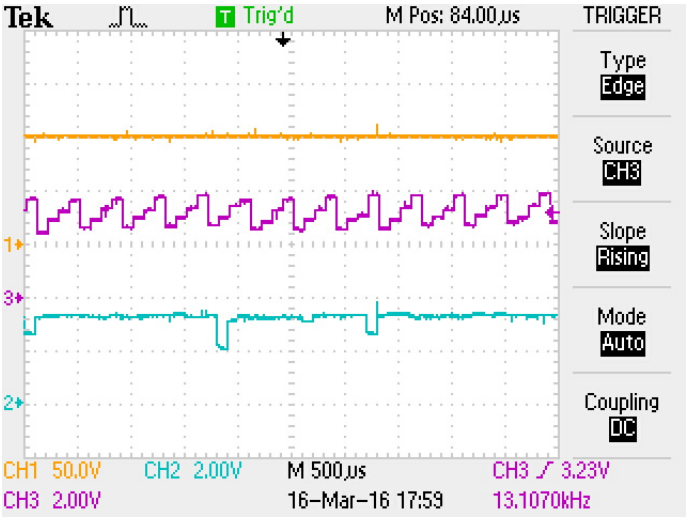

Figure 4.4: V_{DC} controller test in hardware Ch1: DC Bus Voltage V_{DC} controlled at 50V, Ch2: Reference current i_{essref} (A), Ch3: Measured inductor current i_{ess} (A)

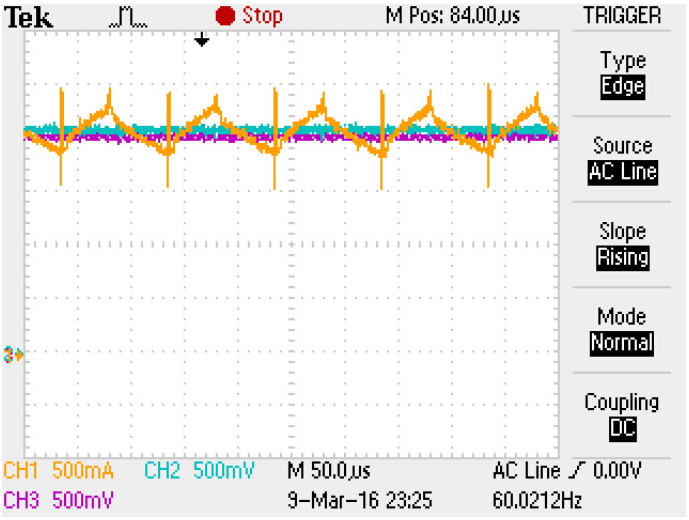

Figure 4.5: i_{rect} controller test in hardware Ch1: Actual inductor current i_{rect} (A), Ch2: Reference current $i_{rectref}$ (A), Ch3: Measured inductor current i_{rect} (A)

4.2.4 PMSG operation using ABB ACS800 drive

PMSG and induction machine are coupled by a mechanical coupler as shown in the Fig. 4.1d. ABB ACS800 drive is first programmed for machine data with appropriate voltage, current, frequency and speed rating of the 3-phase induction motor. It is then programmed to take the analog speed reference in both clockwise and anticlockwise direction. Other motor protection parameters and control parameters are set according to the instruction manual ensuring the safe operation of the drive and motor.

A sinusoidal speed reference is given by DSP to the speed analog input with scale of 1V = 180rpm to ABB ACS800 drive. This causes the induction motor to rotate with corresponding speed and in turn rotate the shaft of the PM synchronous generator. As a result, voltage is generated across the stator terminals of the PMSG and it is show in Fig. 4.6. Figure also shows the rectified output V_{rect}. Note that the stator line voltage values are obtained as analog signals from DSP through voltage sensors. Hence these are scaled to fit the analog output range of -10V to 10V for Oztek DSP.

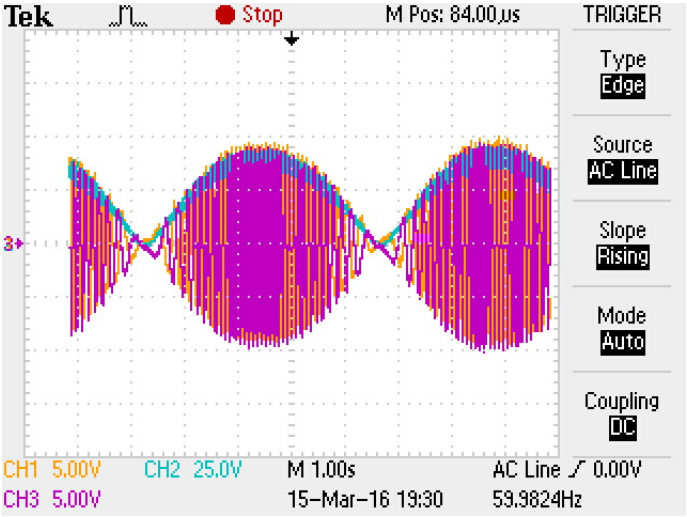

Figure 4.6: PMSG terminal voltage and speed reference, Ch1: Stator line voltage V_{ab} (Scale 1V=3V), Ch2: Rectified voltage V_{rect} (1V), Ch1: Stator line voltage V_{bc} (Scale 1V=3V)

4.2.5 System Setup With DC Supply as ESS

Since all the controllers on the machine side and ESS side boost converters are tested in the previous, we can now connect the system together to form a setup as shown in Fig. 3.15

In this experiment, the ESS voltage is supplied by DC power supply of 48 V. DC Bus voltage is maintained at 90 V. Sinusoidal speed reference of 360rpm peak is given to the drive, which generates rectified voltage output of 45 V. Rectifier current reference is set at 2.3 A peak. Fig 4.7 shows the hardware results for actual rectifier current, DC bus voltage and supercapacitor current.

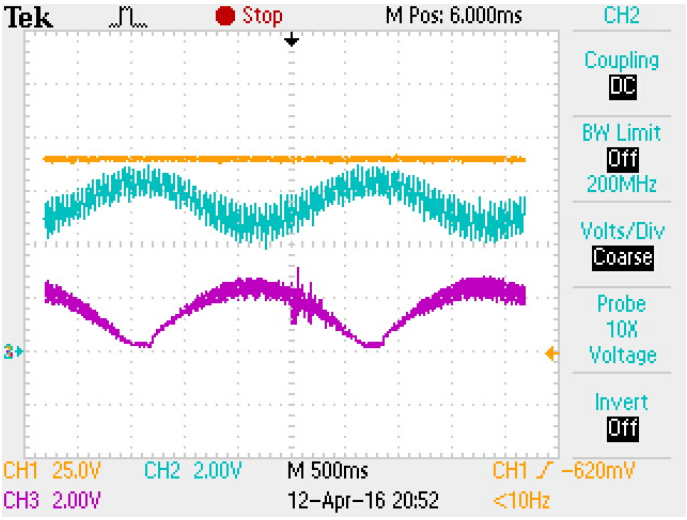

Figure 4.7: System with ESS test in hardware Ch1: DC Bus Voltage V_{DC} controlled at 50V, Ch2: ESS boost inductor current i_{ess} (A), Ch3: Rectifier boost inductor current i_{Rect} (A)

4.2.6 Self excitation for PMSG

Permanent magnet synchronous generator is similar to the induction generator, except that the rotor is replaced by the permanent magnet poles. Therefore, the voltage generated at the stator terminals of the PMSG can be improved by providing reactive power through some external means. Since we are considering stand-alone application of the wave energy generation, reactive power cannot be provided from grid. Hence, self excitation capacitors can be perfect choice [11] - [12]. These capacitors can be connected in parallel with PMSG stator terminal as shown in Fig. 4.8.

Table 4.2: Voltage Compensation of PMSG using self-excitation capacitors

Speed (rpm)	V_{L-LRMS} (V) without C	V_{L-LRMS} with C = 20μF
180	17 V	20 V
360	36 V	38 V
760	54 V	75 V
1500	70 V	170 V

If the rotor of PMSG is rotated by means of induction machine driven by an AC drive, there will be emf induced in the stator winding due to magnetic pole on the rotor. The static capacitors connected in parallel across the stator terminals provide a leading current. This generates flux which assists the original flux. Capacitors of suitable value should be chosen in order to build up the voltage [14].

As the machine is gradually accelerated, the induced voltage suddenly rises after particular speed. After this point, voltage varies monotonically with speed. If the generator is loaded, then the increase in voltage occurs at higher speed.

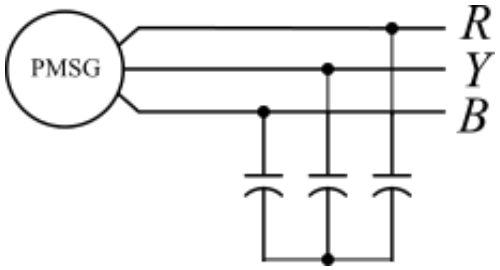

Figure 4.8: Self-excitation capacitor connection for PMSG

C = 20μF capacitors connected in star connection was tested with the available PMSG to achieve higher voltage at the stator terminals. Following table 4.2 shows the distinction between stator terminal voltage with and without self-excitation capacitor. It can be noted that after a particular speed, voltage generated at the terminals increases significantly.

4.2.7 Real time simulation using NI Labview and CompactRIO

Research has been done to find the mechanical dynamics of the WEC with buoy mechanism [15]. Based on these equations, a WEC model is created in the real time simulation environment of NI labview to emulate the WEC system [16]. Labview provides efficient environment for real time simulation.

The model schematic is as shown in Figure 4.9 and 4.10. Sea wave can be considered as combination of various low frequency sinusoidal waves. In this model, actual sea wave data found in realistic survey is used. WEC model provides the torque reference for motor and accepts speed feedback. This torque reference can be provided to the drives of the motor.

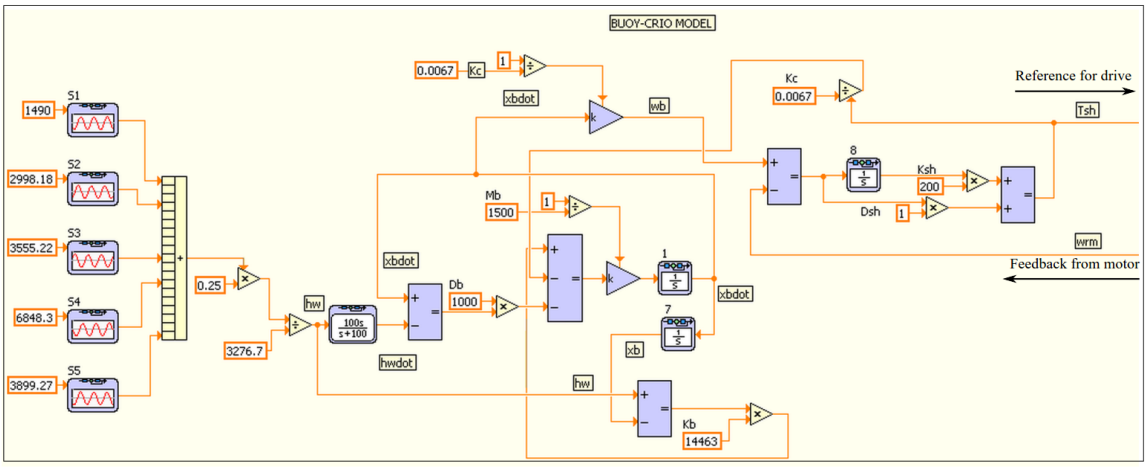

Figure 4.9: Buoy CRIO model in NI Labview

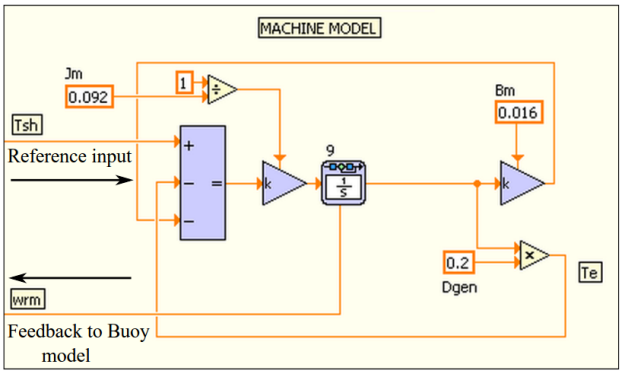

Figure 4.10: Labview and machine model in NI Labview

Chapter 5

Hybrid Energy Storage

Supercapacitors which are also known as ultra-capacitors are being used widely in a variety of power management applications. These supercapacitors have high value of capacitance and the energy is stored electrostatically on the surface of the material [17]. Hence, supercapacitors are having advantage that they can charge-discharge rapidly as compared to the li-ion batteries [18]. Thus, supercapacitors have high power density. But main shortcoming of the supercapacitors is their low energy density, which means the amount of energy that supercapacitors can store per unit weight is very small.

5.1 Supercapacitor

For this system, Maxwell 48V ultracapacitor is used which is shown in Fig. 5.1. Some brief specifications of this supercapacitor are as follows-

Table 5.1: Supercapacitor Specifications

Parameters	Value
Rated Capacitance	83 F
Maximum ESR_{DC}	10 mΩ
Rated Voltage	48 V
Absolute maximum current	1150 A

Figure 5.1: Maxwell 48V supercapacitor module

5.2 Supercapacitor charging and discharging

There are various methods which can be used to charge/discharge supercapacitor [19] - [20]. In this case, constant current constant voltage method is used to charge as well as discharge the supercapacitor [21]. While designing the control for the supercapacitor charging, voltage control cannot be applied initially since it will make supercapacitor draw higher currents from the power supply. Hence, at the start of charging, current control is applied in which supercapacitor voltage is raised from 0 to desired value by charging it with a constant current. As soon as the supercapacitor is charged by constant current to the desired voltage value, voltage control becomes active and it controls the supercapacitor charge level to constant value in order to avoid overcharging.

5.2.1 Constant Current Constant Voltage control

The supercapacitor is charged using a DC power supply which is followed by a DC-DC power converter where only current flow from DC supply will be controlled at first. For this purpose same controller as that of shown in Chapter 3 is used.

For voltage controller, voltage across supercapacitor terminals need to be considered The supercapacitor voltage V_{sc} can be written as,

$$V_{sc}(s) = \frac{I_{sc}(s)}{C_{sc}s}, \tag{5.1}$$

The plant transfer function can be given as follows.

$$G_{I_{scref}}(s) = \frac{1}{C_{sc}s} \tag{5.2}$$

PI controller is designed and Kp,Ki values are appropriately chosen to achieve 1mHz bandwidth for voltage V_{sc}.

$$H_{I_{sc}}(s) = \frac{0.5248(s + 0.001047)}{s} \tag{5.3}$$

The plant transfer function, controller and closed loop gain bode plot is shown in the Fig. 5.2.

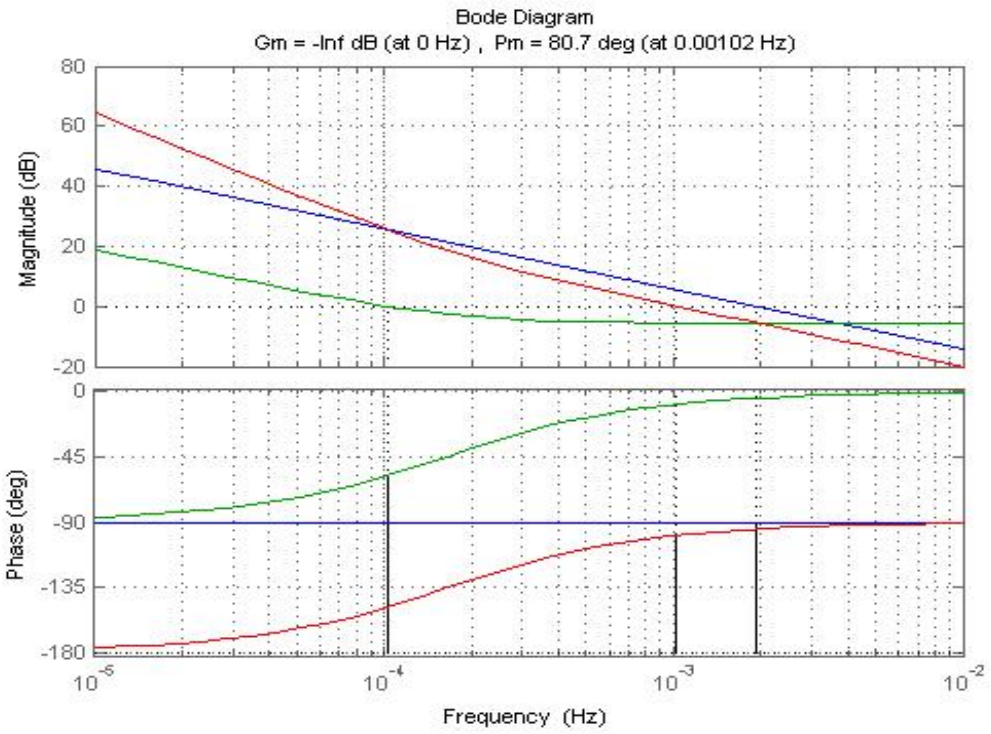

Figure 5.2: V_{sc} control bode plot

5.2.2 Simulation result for charging and discharging of supercapacitor

As discussed earlier, supercapacitor is charged using a DC power supply followed by a DC DC power converter. This is achieved as shown in Fig. 5.3

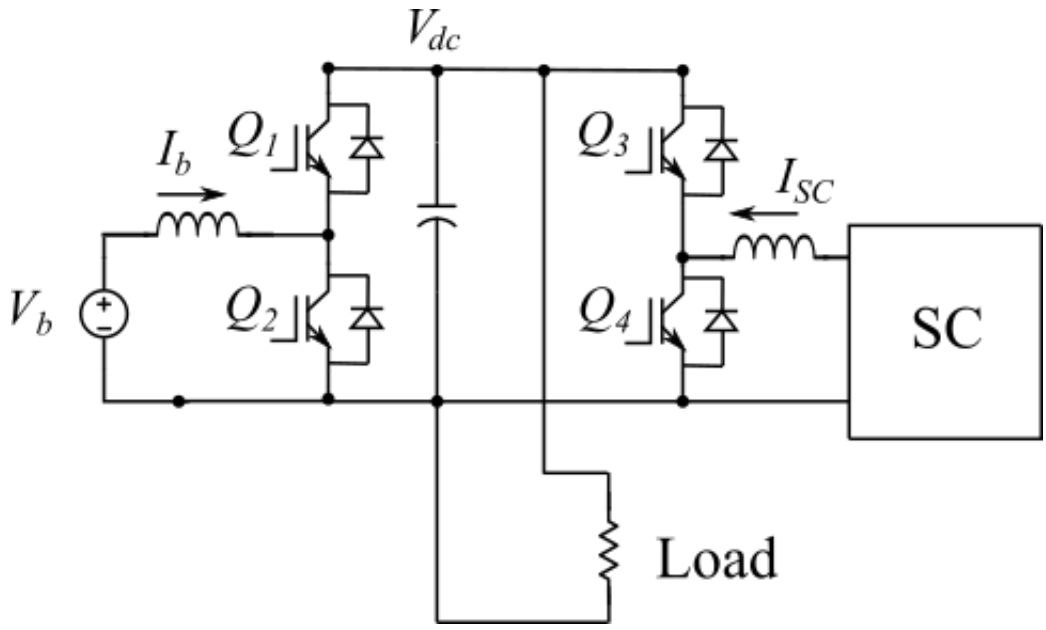

Figure 5.3: Supercapacitor charging schematic

This arrangement shows that in actual system supercapacitor will be used in combination with battery for power smoothing. Hence, we need to use the existing circuit connection to charge the supercapacitor at the start of the system. This can be done by charging the supercapacitor with available battery source.

In this case, only supercapacitor side DC-DC power converter is used for the control. Switch Q1 is kept ON and Q2 is kept off. Current controller will force the required current from battery side to the supercapacitor. Logic for constant current and constant voltage control is designed as shown in the Fig. 5.4.

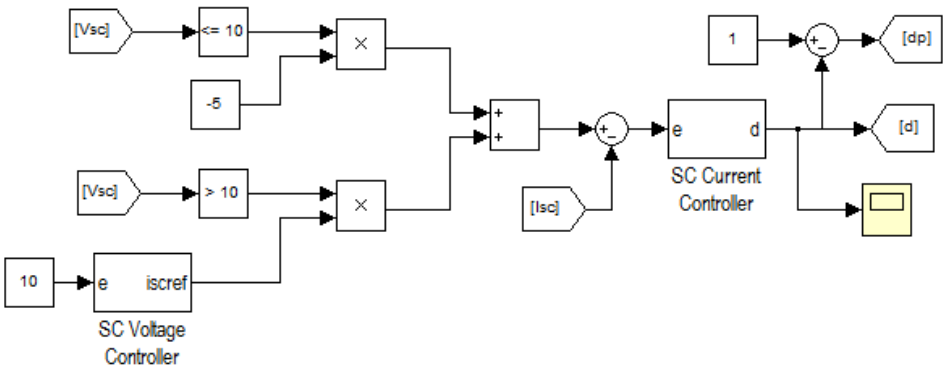

Figure 5.4: Constant current and constant voltage logic

5.2.3 Hardware results for charging and discharging of supercapacitor

As you can see in the Fig. 5.6, the supercapacitor voltage is initially 0V. As soon as the control starts, the reference charging current becomes -5A, where negative sign indicates that the current is flowing into the supercapacitor. The actual inductor current follows this reference current due to current control. In this case, the reference voltage of supercapacitor charging is set at 10V. Hence as soon as the voltage reaches the 10V value, the voltage control becomes active which maintains the supercapacitor voltage at 10V until discharging command is given. Supercapacitor is discharged through a resistive load with SC boost inductor current reference i_{SCref} of 5A. When the supercapacitor voltage falls below 0.5V, it is naturally unable to provide 5A current and gets discharged completely.

5.3 System with supercapacitor

5.3.1 Simulation Results for System with Supercapacitor

Now the ideal voltage source in Fig. 3.15 is replaced by the equivalent supercapacitor of 30V and ESR of 10mΩ. All the ESS controllers discussed so far are used for supercapacitor boost converter. In practical hardware testing, I have kept V_{dc} at 75V. Due to complexity of system, it tends to generate EMI at higher voltages. Hence further simulation results are taken for DC bus voltage of 75V in order to make it comparable with the hardware results. Simulation results are shown in Fig. 5.5. It can be seen that supercapacitor gets discharged quickly in order to supply power mismatch.

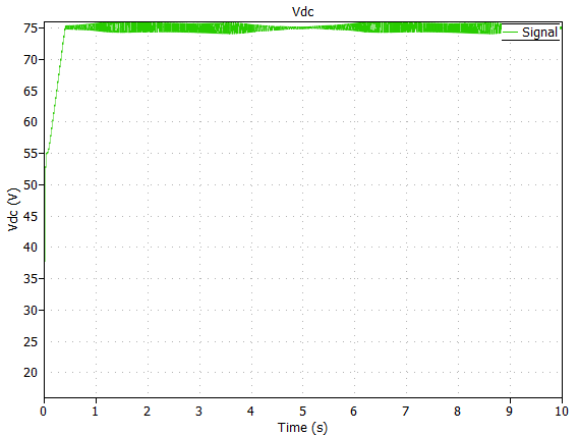

(a) DC Bus Voltage

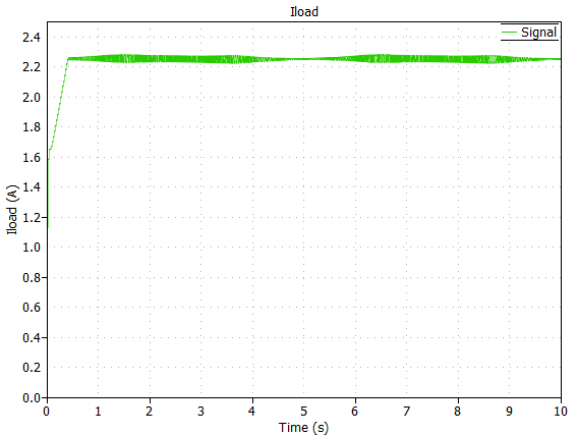

(b) Load Current

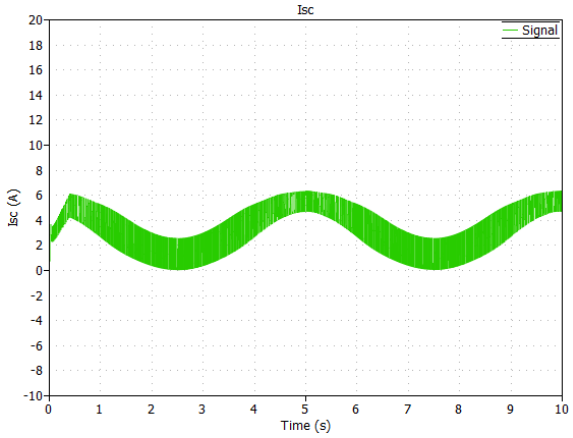

(c) Supercapacitor Current

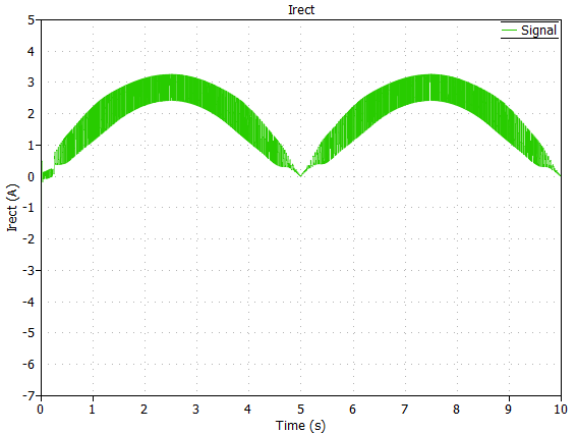

(d) Rectifier Current

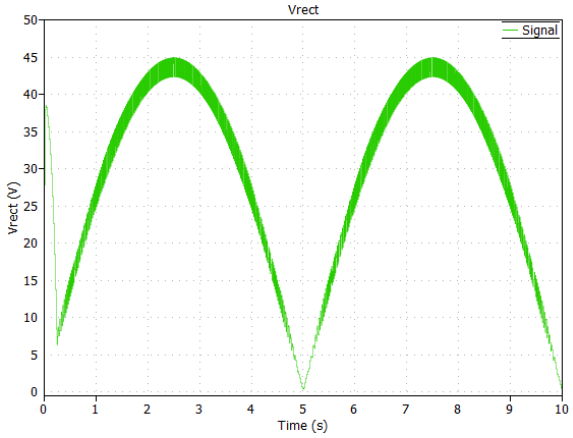

(e) Rectifier Voltage

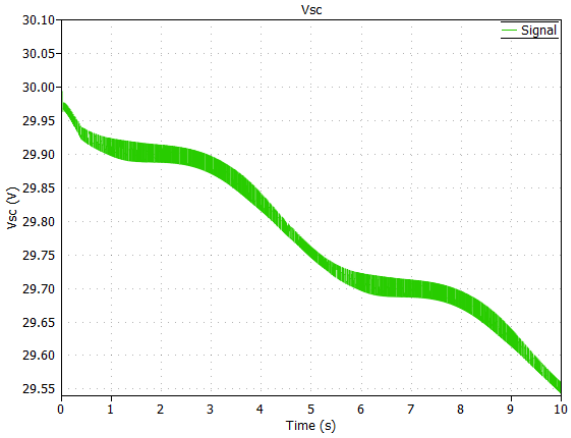

(f) Supercapacitor Voltage

Figure 5.5: Plots for system model with supercapacitor of 30V

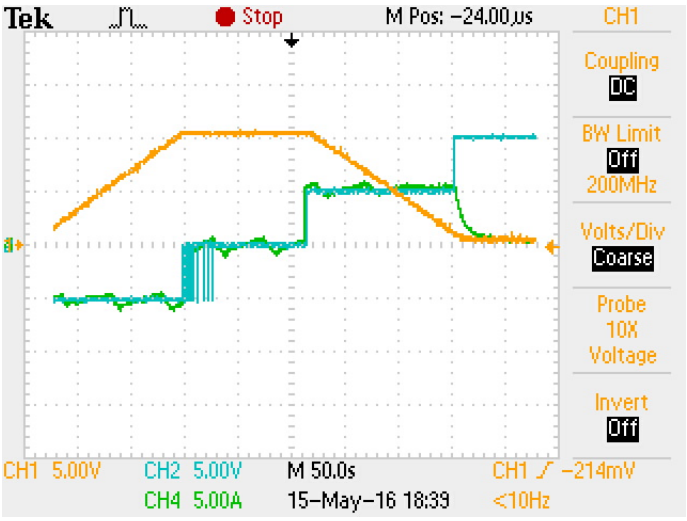

Figure 5.6: Supercapacitor charging-discharging test in hardware Ch1: Supercapacitor Voltage V_{SC} controlled at 10V, Ch2: SC boost inductor reference current i_{SCref} (A), Ch3: SC boost inductor current i_{SC} (A)

5.3.2 System model hardware implementation using supercapacitor

In this experiment, system hardware is experimented by replacing the ideal DC supply with actual supercapacitor. DC bus voltage is regulated at 90V by supercapacitor voltage controller. Since load requirement is 162W or 1.8A which is higher than the average power generated by WEC, supercapacitor eventually discharges as it has to provide the remaining power required by the load. Hence, supercapacitor voltage gradually decreases over the time. Fig. 5.7 shows the plot for the hardware implementation of this system.

5.4 Hybrid energy storage

5.4.1 Difference between supercapacitor and battery

The important difference between supercapacitor and battery is that, the supercapacitor has high power density whereas batteries have high energy density . In other words, supercapacitor is able to give high power in short amount of time. Supercapacitors can handle large number of charge-discharge cycles and can supply very high currents. Hence they are generally used for providing peak powers. Unlike batteries, supercapacitors have almost negligible losses and long lifespan. On the other hand, extracting pulsed power from battery reduces its lifespan. Pulsed current from battery is responsible for transient voltages, increased battery losses and

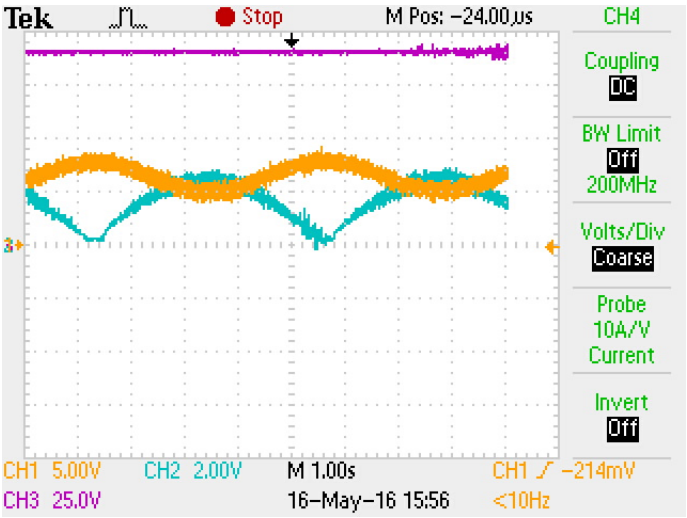

Figure 5.7: System with supercapacitor test in hardware Ch1: SC boost inductor current i_{SC} (1V=1A), Ch1: Ch2: Rectifier boost inductor current i_{Rect} (1V=1A), Ch3: DC Bus Voltage V_{DC} (V)

reduction in battery runtime [22]. Battery also has limitations due to the low charging current as manufacturer's constraint. Hence generally battery is used to provide average power instead of peak power.

5.4.2 Need for hybrid control

So far in the previous chapters, the hardware results were taken by using a DC supply source in replacement of a supercapacitor. But in practical case, the supercapacitor voltage will not remain constant when the load requirement is above the average generated power by WEC. In such cases, the supercapacitor will try to fulfill the requirement of load by discharging the supercapacitor gradually over a period of time. After a certain time, the supercapacitor voltage will not be sufficient enough to regulate the DC bus voltage at desired value and the system will fail. On contrary, if the load requirement is much lower than the average power generated by WEC, then the supercapacitor will overcharged when the generated power is higher than load requirement. This will cause the supercapacitor voltage to rise beyond the maximum voltage that supercapacitor can handle.

This overcharging or discharge of supercapacitor happens because the supercapacitor current in such cases oscillates over an average current. If we can make this average current, then the charging current will be equal to the discharging current. Hence, supercapacitor voltage will get maintained at same voltage level. To achieve this state, it becomes necessary to make use of

hybrid control of battery along with the supercapacitor. Since battery has high energy density, it has slow charging and discharging rate. This advantage of battery can be used to provide the average power which was previously being provide by supercapacitor alone.

5.4.3 Control and simulation of battery current

Apart from providing the average current, battery also need to operate in such a way that it does not let the supercapacitor voltage value to cross beyond limits. Hence we need one current controller as well as voltage controller.

We can write the voltage across the battery side inductor L_b as

$$d_b V_{dc} - V_b = I_b L_b s \tag{5.4}$$

Here V_{dc} is the output DC voltage which is controlled by SC boost converter, I_b is the battery boost converter inductor current, d_{sc} is the duty ratio of the SC boost. Since V_b is the disturbance input, the transfer function can be given as follows.

$$G_{I_b}(s) = \frac{I_b(s)}{d_b(s)} = \frac{V_{dc}}{L_b s} \tag{5.5}$$

PI controller is designed and Kp,Ki values are appropriately chosen to achieve 600Hz bandwidth for current I_b. This controller is chosen to be with higher bandwidth in order to give quick response.

$$H_{I_b}(s) = \frac{0.0188(s + 628.19)}{s} \tag{5.6}$$

The plant transfer function, controller and closed loop gain bode plot for I_b is shown in the Fig. 5.8.

The current reference for battery will be obtained from supercapacitor terminal voltage as well as the average power requirement. Average power requirement can be calculated by using a low pass filter. Low pass filter transfer function can be given as follows,

$$H_{LPF}(s) = \frac{1}{1 + s/\omega_c} \tag{5.7}$$

Since, we want to get the average of entire supercapacitor current reference, taking exact cut-off frequency of supercapacitor reference current frequency will not be sufficient. Hence, larger time period of 100 sec is considered. This gives cut off frequency of 0.01 Hz. This consideration is very important since average current reference with only 0.01 Hz frequency variation is allowed to pass through.

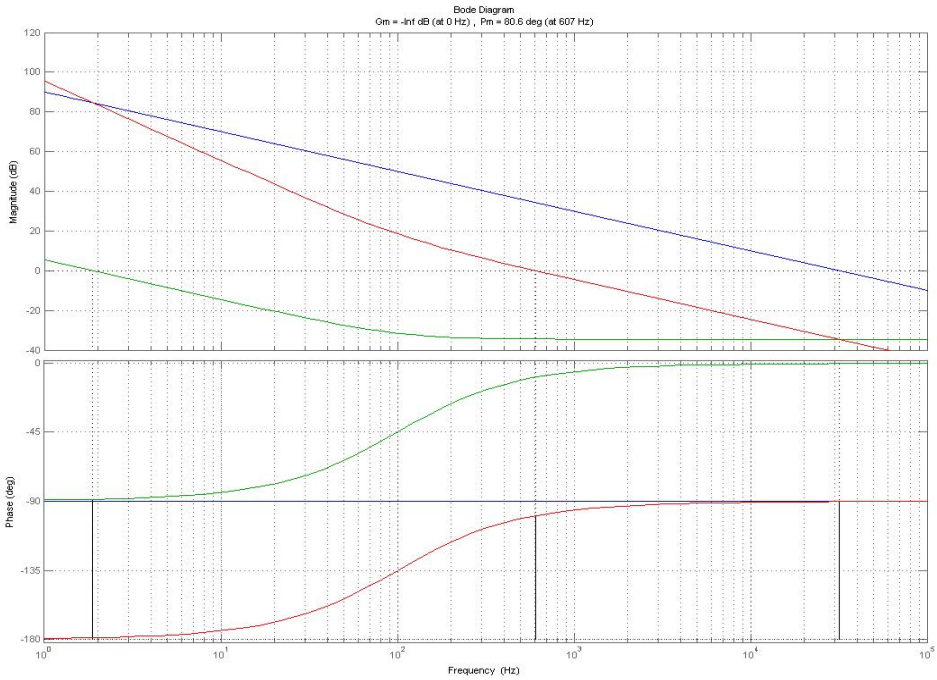

Figure 5.8: I_b control bode plot

$$\begin{aligned} \omega_c &= 2\pi f_c && (5.8)\\ &= 2\pi 0.01 && (5.9)\\ H_{LPF}(s) &= \frac{1}{1+s/\omega_c} && (5.10) \end{aligned}$$

Hence the battery current reference based on average power requirement can be written as,

$$I_{essref\_LF}(s) = H_{LPF}(s) * i_{essref}(s) \tag{5.11}$$

Voltage across the supercapacitor C_{sc} can be written as

$$\begin{aligned} V_{sc}(s) &= \frac{I_{sc}(s)}{C_{sc}s}, && (5.12)\\ V_{sc}(s) &= \frac{1}{C_{sc}s} I_{batref\_vsc}(s) && (5.13) \end{aligned}$$

By providing I_{batref_vsc}, battery will try to limit the supercapacitor terminal voltage. The plant

transfer function can be given as follows.

$$G_{i_{batref\_vsc}}(s) = \frac{V_{sc}(s)}{I_{batref2}(s)} = \frac{1}{C_{sc}s} \tag{5.14}$$

Proportional controller is designed and Kp value is appropriately chosen to achieve 0.01Hz bandwidth for controlling voltage v_{sc}.

$$H_{i_{batref\_vsc}}(s) = 5.188 \tag{5.15}$$

The plant transfer function, controller and closed loop gain bode plot for V_{sc} control is shown in the Fig. 5.9.

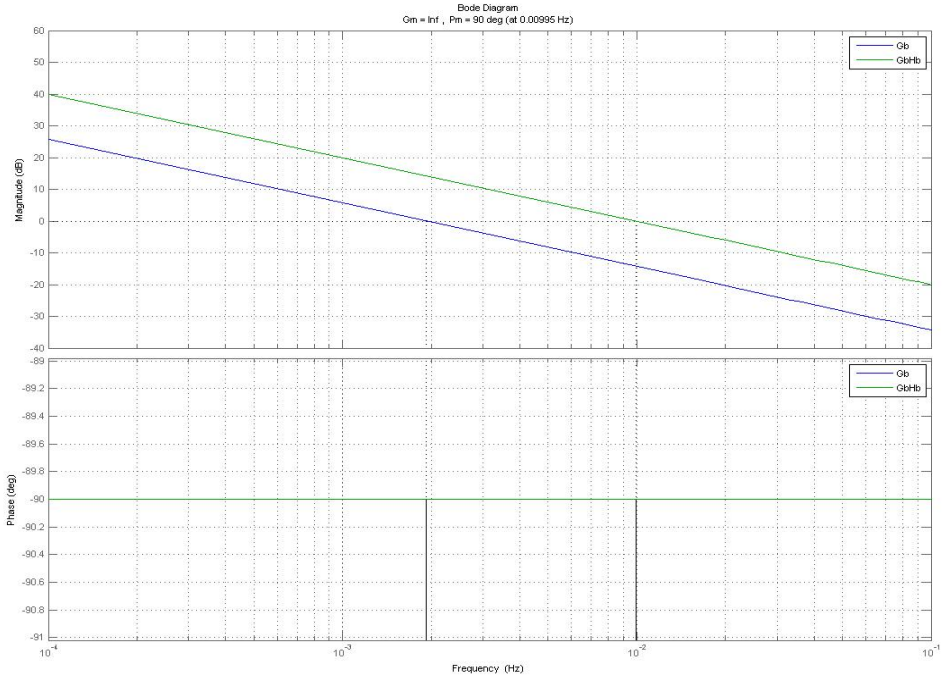

Figure 5.9: v_{sc} control bode plot

We can add the reference currents for battery obtained from both V_{sc} controller and low pass filter to give the total battery reference current.

$$I_{batref} = i_{essref\_LF} + I_{batref\_vsc} \tag{5.16}$$

5.4.4 System model simulation of hybrid supercapacitor and battery control

To provide average current by using battery, a simple low pass filter is used. Reference current generated for supercapacitor by voltage controller is passed through this low pass filter to give average current. Fig. 5.10 is modeled in Simulink for simulation purpose. Controller block diagram for hybrid control is as shown in Fig. 5.12

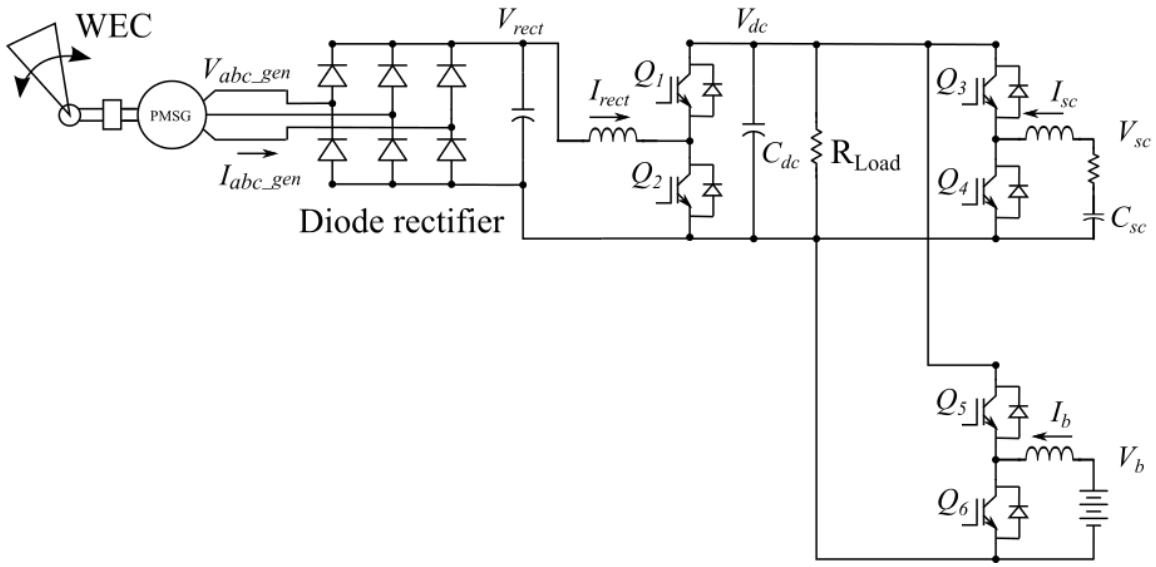

Figure 5.10: System circuit with hybrid battery and supercapacitor

Simulation is carried out for sinusoidal speed reference of 360rpm. As shown in Fig. 5.11, this generates V_{rect} of 46V. I_{rect} is controlled in proportion to the speed reference. Resistive load of 33 Ω is connected to the DC bus. DC bus voltage is regulated at 75 V using supercapacitor voltage controller. Hence load power requirement is around 2.3 A. As system starts running, initially battery is not supplying any power and hence supercapacitor starts discharging and fulfills the power requirement. Gradually, due to combination of low pass filter and supercapacitor terminal voltage controller battery starts to supply average power requirement. Hence, supercapacitor current which was previously oscillating over some average current starts decreasing and starts oscillating over zero axis. Thus we can see that equilibrium is achieved and supercapacitor voltage is maintained by equal and alternate charge discharge cycles.

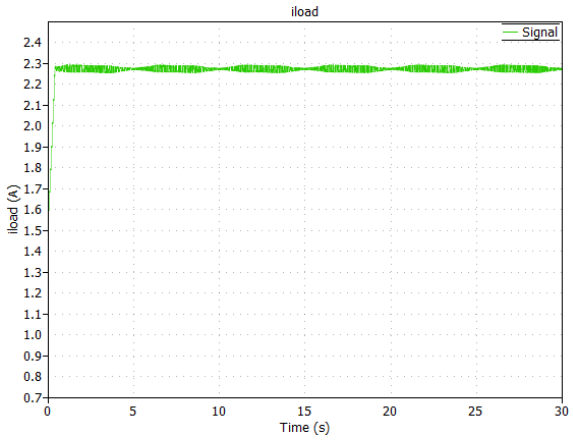

(a) Load current

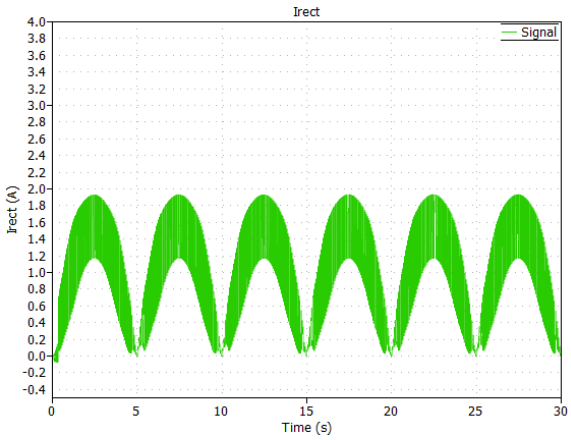

(b) Rectified Current

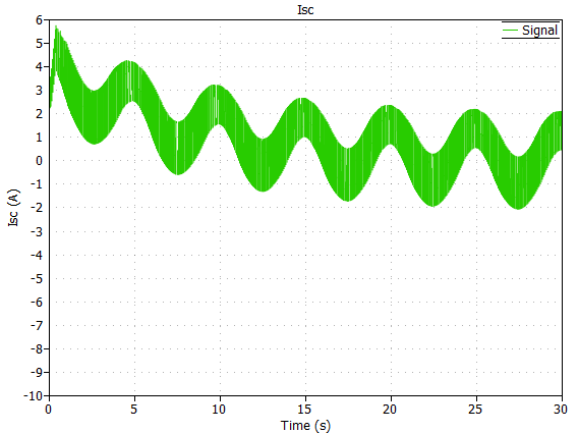

(c) Supercapacitor Current

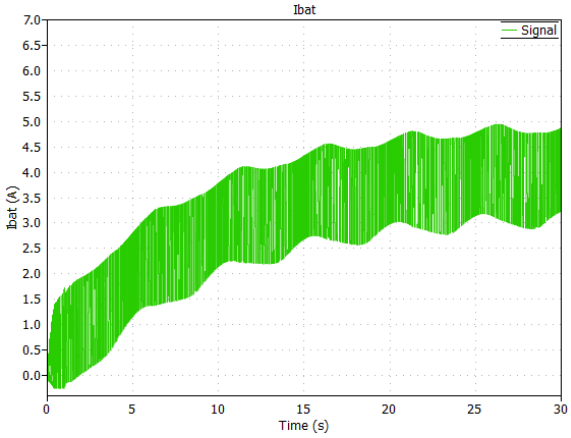

(d) Battery Current

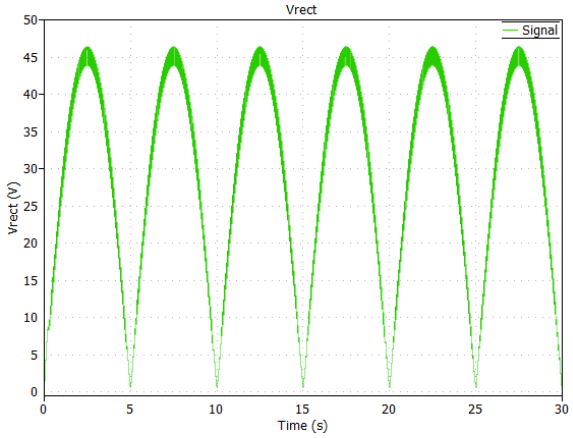

(e) Rectifier Voltage

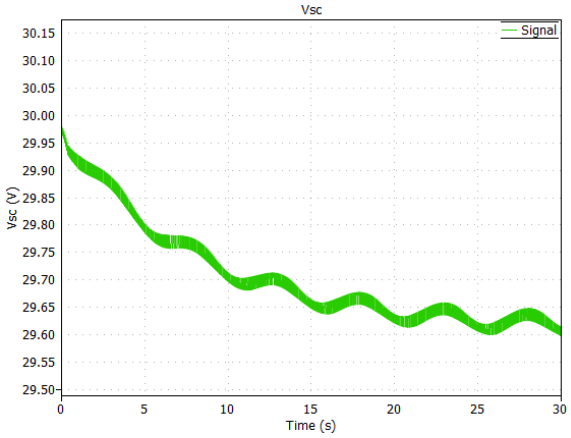

(f) Supercapacitor Voltage

Figure 5.11: Plots for system model with hybrid battery and supercapacitor control

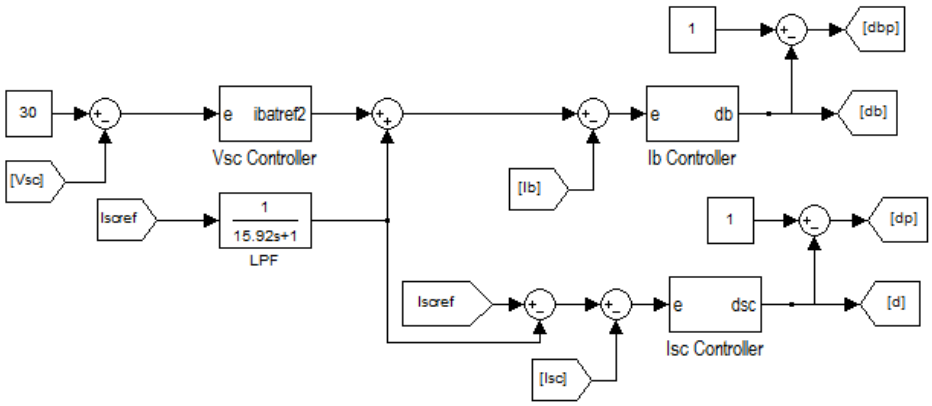

Figure 5.12: Hybrid battery and supercapacitor controller

5.4.5 System model hardware implementation using hybrid supercapacitor and battery control

A bi-directional boost converter and battery supply is added in the hardware to the setup which was used earlier in Chapter 4. Complete hardware setup is built as shown in Fig. 5.13. During experiment, supercapacitor is first charged upto 30 V using constant current and constant voltage control. Once supercapacitor is charged, system is turned on using relay logic and SC side boost converter is operated to regulate DC bus voltage at 75V. This also triggers an analog signal through DSP which acts as sinusoidal speed reference of 360rpm peak for ABB drive. This causes PMSG to generate 3-phase voltage at its terminals and system runs only with supercapacitor. As shown in Fig. 5.14, for initial 10 sec period supercapacitor current has average of 6 A. After 10 secs, battery side power converter is operated. In practical situation, supercapacitor voltage reduces slightly from 30 V to 28-29 V before we start battery side power converter. Hence, supercapacitor terminal voltage reference is kept at 28 V in order to draw reasonable current from battery for controlling supercapacitor voltage. As the battery starts providing the average power requirement, supercapacitor current average reduces and it starts oscillating on zero axis. This means battery is successfully providing average power requirement and peak power is achieved using supercapacitor.

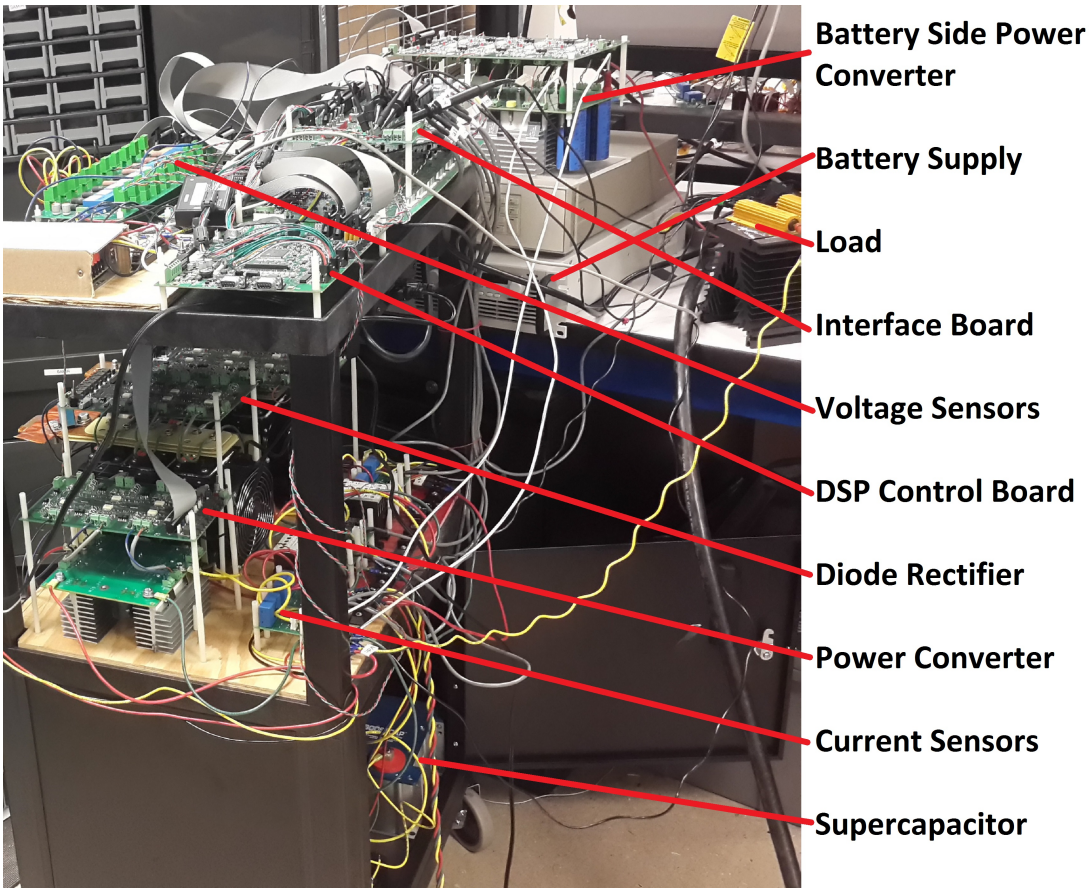

Figure 5.13: Hardware setup for wave energy generation with hybrid energy storage

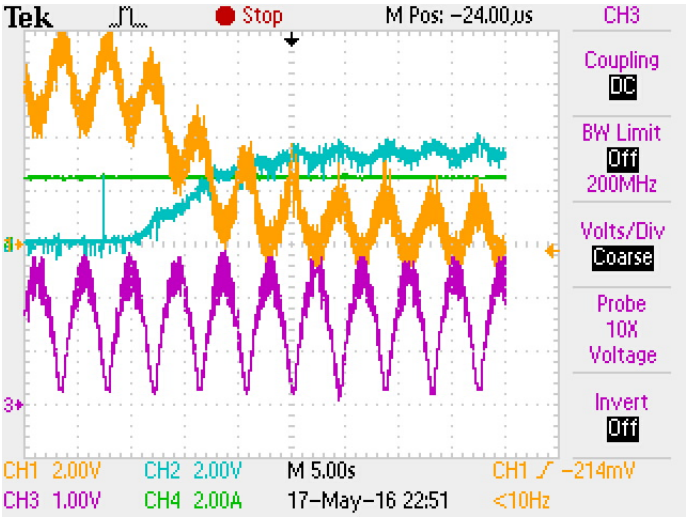

Figure 5.14: System with hybrid energy storage test in hardware Ch1: Supercapacitor current I_{SC} (1V=1A), Ch2: Battery current I_b (1V=1A) Ch3: Rectifier current I_{Rect} (1V=1A), Ch4: Load current I_{Rect} (1V=1A)

5.5 Conclusion

This thesis discussed the integration of hybrid energy storage in oscillatory wave energy generation system to provide smooth power in stand-alone application. Low cost is achieved by use of diode rectifier as compared to active converter. Hybrid energy storage control is achieved using supercapacitor and DC power supply as battery. Simulation and hardware results are obtained to demonstrate the output power smoothing for resistive load. Hardware results are comparable with the simulation results and it can be seen that hybrid energy storage control is successully achieved. It can be seen that the supercapacitor current intially in hardware result is slightly higher than the one obtained in simulation. This is because in simulation battery current starts gradually increasing as soon as the simulation is started which reduces power requirement from the supercapacitor. But in practical case, battery side boost converter is operated after some delay.

Future work can be done by replacing DC supply with actual battery and including practical conditions associated with battery charge-discharge.

REFERENCES

[1] B. Czech and P. Bauer, "Wave Energy Converter Concepts : Design Challenges and Classification" *in IEEE Industrial Electronics Magazine*, vol. 6, no. 2, pp. 4-16, June 2012.

[2] K. Edwards and M. Mekhiche, "Ocean power technologies powerbuoy: System-level design, development and validation methodology" *in Proc. Marine Energy Tech. Symp.(METS)* Seattle, WA, USA, 2014.

[3] S. Hazra, S. Bhattacharya, K. K. Uppalapati, and J. Bird, "Ocean energy power take-off using oscillating paddle" *Proc. IEEE Energy Convers. Congr. and Expo. (ECCE)*, Raleigh, NC, USA, 2012, pp. 407413.

[4] L. Cameron, R. Doherty, A. Henry, K. Doherty, J. Vant Hoff, D. Kaye, D. Naylor, S. Bourdier, and T. Whittaker, "Design of the next generation of the oyster wave energy converter" *in Proc. IEEE Int. Conf. on Ocean Energy (ICOE)*, vol. 6, Bilbao, Spain, 2010.

[5] S. Hazra and S. Bhattacharya, "Electrical machines for power generation in oscillating wave energy conversion system A comparative study" *in 2015 IEEE International Electric Machines and Drives Conference*, Coeur d'Alene, ID, 2015, pp. 1538-1544.

[6] S. Hazra and S. Bhattacharya, "Short time power smoothing of a low power wave energy system" *IECON 2012 – 38th Annual Conference on IEEE Industrial Electronics Society*, Montreal, QC, 2012, pp. 5846-5851.

[7] C. Siqi et al. "Optimal coordinated operation for microgrid with hybrid energy storage and diesel generator" *in Power System Technology (POWERCON)*, 2014 International Conference on, Chengdu, 2014, pp. 3207-3212.

[8] H. Lee, B. Y. Shin, S. Han, S. Jung, B. Park and G. Jang, "Compensation for the Power Fluctuation of the Large Scale Wind Farm Using Hybrid Energy Storage Applications" *in IEEE Transactions on Applied Superconductivity*, vol. 22, no. 3, pp. 5701904-5701904, June 2012.

[9] J. Deng, J. Shi, Y. Liu and Y. Tang, "Application of a hybrid energy storage system in the fast charging station of electric vehicles" *in IET Generation, Transmission & Distribution*, vol. 10, no. 4, pp. 1092-1097, 3 10 2016.

[10] Robert W. Erickson, Dragan Maksimovic, "Fundamentals of Power Electronics" *2nd edition*, 2004, Kluwer Academic Publishers

[11] Dandan Ma, "Vector oriented control of voltage source PWM inverter as a dynamic VAR compensator for wind energy conversion system connected to utility grid" *in Doctor of Philosophy Thesis*, Newcastle University, United Kingdom, May, 2012.

[12] M. M. N. Amin and O. A. Mohammed, "Self-excited Induction Generator A Study Based on Nonlinear Dynamic Methods" *in Applied Power Electronics Conference and Exposition (APEC), 2010 Twenty-Fifth Annual IEEE*, Palm Springs, CA, 2010, pp. 1640-1650.

[13] J. Arrillaga and D. B. Watson, "Static power conversion from self-excited induction generators" *in Proceedings of the Institution of Electrical Engineers*, vol. 125, no. 8, pp. 743-746, August 1978.

[14] E. Bim, J. Szajner and Y. Burian, "Voltage compensation of an induction generator with long-shunt connection" *in IEEE Transactions on Energy Conversion*, vol. 4, no. 3, pp. 526-530, Sep 1989.

[15] S. Hazra, A. S. Shrivastav, A. Gujarati and S. Bhattacharya "Dynamic emulation of oscillating wave energy converter" *in 2014 IEEE Energy Conversion Congress and Exposition (ECCE)*, Pittsburgh, PA, 2014, pp. 1860-1865.

[16] Samir Hazra, Prathamesh Kamat, Ashish Shrivastav, Subhashish Bhattacharya, "Emulation of oscillating wave energy converter for laboratory test bed" *in Marine Energy Technology Symposium*, April 27-29, 2015, Washington, DC.

[17] https://en.wikipedia.org/wiki/Supercapacitor

[18] V. Musolino, E. Tironi and P. di Milano, "A comparison of supercapacitor and high-power lithium batteries" *in Electrical Systems for Aircraft, Railway and Ship Propulsion*, Bologna, 2010, pp. 1-6.

[19] S. Sikkabut et al., "Comparative study of control approaches of Li-Ion battery/supercapacitor storage devices for fuel cell power plant," *in 2015 International Conference on Clean Electrical Power (ICCEP)*, Taormina, 2015, pp. 647-652.

[20] L. Jiang and B. J. Arnet, "Charging Supercapacitors from Low Voltage with an Induction Machine" *in 2007 IEEE Vehicle Power and Propulsion Conference*, Arlington, TX, 2007, pp. 537-543.

[21] http://www.intersil.com/content/dam/Intersil/whitepapers/switching-controller/supercapacitor-charging.pdf

[22] A. Lahyani, P. Venet, A. Guermazi and A. Troudi, "Battery/Supercapacitors Combination in Uninterruptible Power Supply (UPS)" *in IEEE Transactions on Power Electronics*, vol. 28, no. 4, pp. 1509-1522, April 2013.